

## Effect of formal and informal likelihood functions on uncertainty assessment in a single event rainfall-runoff model



Mahrouz Nourali<sup>a</sup>, Bijan Ghahraman<sup>b,\*</sup>, Mohsen Pourreza-Bilondi<sup>c</sup>, Kamran Davary<sup>b</sup>

<sup>a</sup> Department of Water Engineering, Faculty of Agriculture, Ferdowsi University of Mashhad, International Campus, Mashhad, Iran

<sup>b</sup> Department of Water Engineering, Faculty of Agriculture, Ferdowsi University of Mashhad, Mashhad, Iran

<sup>c</sup> Department of Water Engineering, College of Agriculture, University of Birjand, Birjand, Iran

### ARTICLE INFO

#### Article history:

Received 5 June 2016

Accepted 10 June 2016

Available online 17 June 2016

This manuscript was handled by Andras Bardossy, Editor-in-Chief, with the assistance of Jozsef Szilagyi, Associate Editor

#### Keywords:

Uncertainty

DREAM<sub>(ZS)</sub>algorithm

Formal/ Informal likelihood function

HEC-HMS

First-order autoregressive

### ABSTRACT

In the present study, DREAM<sub>(ZS)</sub>, Differential Evolution Adaptive Metropolis combined with both formal and informal likelihood functions, is used to investigate uncertainty of parameters of the HEC-HMS model in Tamar watershed, Golestan province, Iran.

In order to assess the uncertainty of 24 parameters used in HMS, three flood events were used to calibrate and one flood event was used to validate the posterior distributions. Moreover, performance of seven different likelihood functions (L1–L7) was assessed by means of DREAM<sub>(ZS)</sub> approach. Four likelihood functions, L1–L4, Nash–Sutcliffe (NS) efficiency, Normalized absolute error (NAE), Index of agreement (IOA), and Chiew–McMahon efficiency (CM), is considered as informal, whereas remaining (L5–L7) is represented in formal category. L5 focuses on the relationship between the traditional least squares fitting and the Bayesian inference, and L6, is a heteroscedastic maximum likelihood error (HMLE) estimator. Finally, in likelihood function L7, serial dependence of residual errors is accounted using a first-order autoregressive (AR) model of the residuals.

According to the results, sensitivities of the parameters strongly depend on the likelihood function, and vary for different likelihood functions. Most of the parameters were better defined by formal likelihood functions L5 and L7 and showed a high sensitivity to model performance. Posterior cumulative distributions corresponding to the informal likelihood functions L1, L2, L3, L4 and the formal likelihood function L6 are approximately the same for most of the sub-basins, and these likelihood functions depict almost a similar effect on sensitivity of parameters. 95% total prediction uncertainty bounds bracketed most of the observed data. Considering all the statistical indicators and criteria of uncertainty assessment, including RMSE, KGE, NS, P-factor and R-factor, results showed that DREAM<sub>(ZS)</sub> algorithm performed better under formal likelihood functions L5 and L7, but likelihood function L5 may result in biased and unreliable estimation of parameters due to violation of the residual error assumptions. Thus, likelihood function L7 provides posterior distribution of model parameters credibly and therefore can be employed for further applications.

© 2016 Elsevier B.V. All rights reserved.

## 1. Introduction

During the past decades, conceptual rainfall-runoff models have been extensively used for watershed management policies and operational and research purposes. Uncertainty in model predictions are caused by the natural randomness, the measurement

errors in input (forcing) and output data, the uncertainty in model parameters and the model structure (Blasone, 2007; Alazzy et al., 2015). Hydrologic models often include parameters that cannot be measured directly, so parameter estimation through calibration process is prone to error because the data, which were employed for calibration, generally contain measurement errors (Vrugt et al., 2003). Therefore, accurate calibration and uncertainty analysis is an important step for these models (Beven, 2006).

In order to estimate predictive uncertainty of the hydrologic models, infer the parameters, and predict model outputs, various methodologies may be adopted, including first-order approximation (Kool and Parker, 1988; Vrugt and Bouten, 2002), state-space filtering (Salamon and Feyen, 2009; DeChant and

\* Corresponding author at: Department of Water Engineering, Faculty of Agriculture, Ferdowsi University of Mashhad, Mashhad, Iran. Tel.: +98 513 8805709; fax: +98 513 8807145.

E-mail addresses: [mahrouznourali@yahoo.com](mailto:mahrouznourali@yahoo.com) (M. Nourali), [bijangh@um.ac.ir](mailto:bijangh@um.ac.ir) (B. Ghahraman), [mohsen.pourreza@birjand.ac.ir](mailto:mohsen.pourreza@birjand.ac.ir) (M. Pourreza-Bilondi), [kam dav@um.ac.ir](mailto:kam dav@um.ac.ir) (K. Davary).

Moradkhani, 2012; Vrugt et al., 2013), multi model averaging (Ajami et al., 2007; Vrugt and Robinson, 2007), and various Bayesian approaches (Kavetski et al., 2006a,b; Kuczera et al., 2006; Reichert and Mieleitner, 2009; Renard et al., 2011; Rings et al., 2012; Vrugt et al., 2008, 2009b).

Among these approaches, Bayesian statistics have been widely used in hydrology for statistical inference of parameters and model output prediction (Kuczera and Parent, 1998; Bates and Campbell, 2001; Vrugt et al., 2003; Marshall et al., 2004; Liu and Gupta, 2007). Under Bayes theorem, posterior distribution combines the data likelihood with the prior distributions of parameters.

In majority of hydrological models, posterior distribution cannot be estimated by analytical approximation and, hence, simulation methods such as Markov chain Monte Carlo (MCMC) sampling can be adopted to implement Bayesian approach successfully. This method can efficiently estimate posterior probability density function (pdf) of the parameters.

MCMC methods are stochastic simulation algorithms that successively meet the solutions in parameter space, where solutions finally converge to posterior probability distributions. For any situation, different approaches of MCMC samplers may be considered by using suitable sampling or proposed distribution, while the convergence to the target posterior distribution is guaranteed (Vrugt et al., 2003; Blasone, 2007).

In hydrologic studies, in order to estimate parameter uncertainty of the hydrologic models, a suitable likelihood function has to be considered which provides reliable parameters of model. Formal or informal likelihood functions in Bayesian approaches have been used to estimate parameter uncertainty (Mantovan and Todini, 2006; Beven et al., 2008; Stedinger et al., 2008; McMillan and Clark, 2009; Vrugt et al., 2009b; Cheng et al., 2014). Formal likelihood functions are derived from an assumed statistical model for the residual errors (Box and Tiao, 1992). For example, the standard least squares (SLS) approach is used to derive the formal likelihood function under the assumptions that error residuals are uncorrelated (independent) and identically distributed by normal or Gaussian distribution with zero mean and constant variance (e.g. Vrugt et al., 2009b).

This approach is criticized, as it is highly depended on the assumptions of the residual error (Beven et al., 2008; Thyer et al., 2009), while in fact in many cases residual errors are correlated (dependent), nonstationary (heteroscedasticity), and non-Gaussian distributed (Kuczera, 1983). Revoking SLS assumptions may result in biased estimations of the parameters and affect either parameter or prediction uncertainties.

Informal likelihood functions are subjective likelihood probabilities and are not derived from a known model for the stochastic error series (Smith et al., 2008). For example Generalized Likelihood Uncertainty Estimation method (GLUE) (Beven and Binley, 1992), presented in the hydrologic literature, is often applied with a statistically informal likelihood function (Vrugt et al., 2009b). An informal approach may be used to estimate the uncertainty interval, where traditional error assumptions are violated. But this approach does not adhere to the formal statistical principles, and an informal likelihood function is not explicitly linked to an underlying error model (Schoups and Vrugt, 2010).

Choosing likelihood function requires a reasonable description of the distribution of the model errors in order to estimate the parameters, uncertainties and the statistical inferences accurately (He et al., 2010). If a likelihood function is arbitrarily applied that does not reasonably represent the distribution of the model errors, the results are unreliable.

When the assumptions of the residual error are violated, formal likelihood function must be applied based on a general error model. The general error model allows for the model bias and the correlation; nonstationarity (heteroscedasticity) and the

nonnormality of the model residuals (e.g. Schoups and Vrugt, 2010). In addition, various methods may be used to relax common assumptions about residual errors, e.g. Box-Cox transformations to induce homoscedasticity (constant variance) and a first-order autoregressive (AR-1) scheme of the residuals to remove the temporal autocorrelation (e.g. Sorooshian and Dracup, 1980; Bates and Campbell, 2001).

Residuals of the rainfall-runoff models are often autocorrelated, because of the observed data and model structural uncertainties (Laloy et al., 2010). To account for the correlated errors, one common applied approach is using a first-order autoregressive (AR) scheme of the error residuals and considering the effect of model structural error (Vrugt et al., 2009b).

The hydrological modeling literature has mostly focused on the effect of choosing a likelihood function on the uncertainty analysis in the GLUE method and has showed that selection of likelihood function can directly affect the uncertainty analysis and the sensitivity of parameters (e.g. Freer et al., 1996; Stedinger et al., 2008; Freni et al., 2009; Alazzy et al., 2015).

Recently, a new Markov chain Monte Carlo (MCMC) sampler, namely DREAM<sub>(ZS)</sub> (DiffeRential Evolution Adaptive Metropolis algorithm), was used under a Bayesian framework as an efficient and robust sampler. Compared to the generalized likelihood uncertainty estimation (GLUE), the main advantage of DREAM (using MCMC simulation) is separating the effects of input (forcing), parameters and model structural uncertainties from total predictive uncertainty (Vrugt et al., 2009b).

DREAM<sub>(ZS)</sub> is based on the original DREAM algorithm (Vrugt et al., 2009a) that was modified for an efficient estimation of the posterior probability density function of parameters of a complex hydrologic model, high-dimensional posterior exploration problems.

Since results which are influenced by different likelihood functions, are important and considerable, this research demonstrates the importance and impact of choosing likelihood function on the parameter posterior distributions in a single event based rainfall-runoff model (HEC-HMS).

So, the influences of four informal likelihood functions and three formal likelihood functions were evaluated on estimating the parameters of HEC-HMS under DREAM<sub>(ZS)</sub> framework.

In this paper, study area is briefly described, and then the hydrologic model is presented. Afterwards, details of the procedures used to implement DREAM<sub>(ZS)</sub> method with different likelihood functions in the HEC-HMS hydrologic model are fully explained. Then the description of criteria is followed which are used to compare the effects of likelihood functions on the results of DREAM<sub>(ZS)</sub> method. Finally, the results and discussion are presented which are followed by a summary of the most important conclusions of this study.

## 2. Materials and methods

### 2.1. Case study and data

The study area is located in Gorganroud river basin, Golestan province, Iran, with an area of 3626.5 km<sup>2</sup> and is divided into three sub-basins, Tamar, Tangrah, and Galikesh, with areas of about 1530, 1724 and 372.5 km<sup>2</sup>, respectively. In the study area, flash floods occasionally occur which cause some damages to lives, so flood control management plans are urgent in the basin. Annual rainfall varies between 200 and 850 mm in the basin (IWRI, 2008).

In the present study, Tamar basin was selected due to the availability of more reliable data of this basin. This basin is located between longitudes from 55°30'00" to 56°04'37"E and latitudes from 37°24'49" to 37°47'48"N (Fig. 1). The elevation of the basin ranges from 113 m at the basin outlet to about 2160 m at the

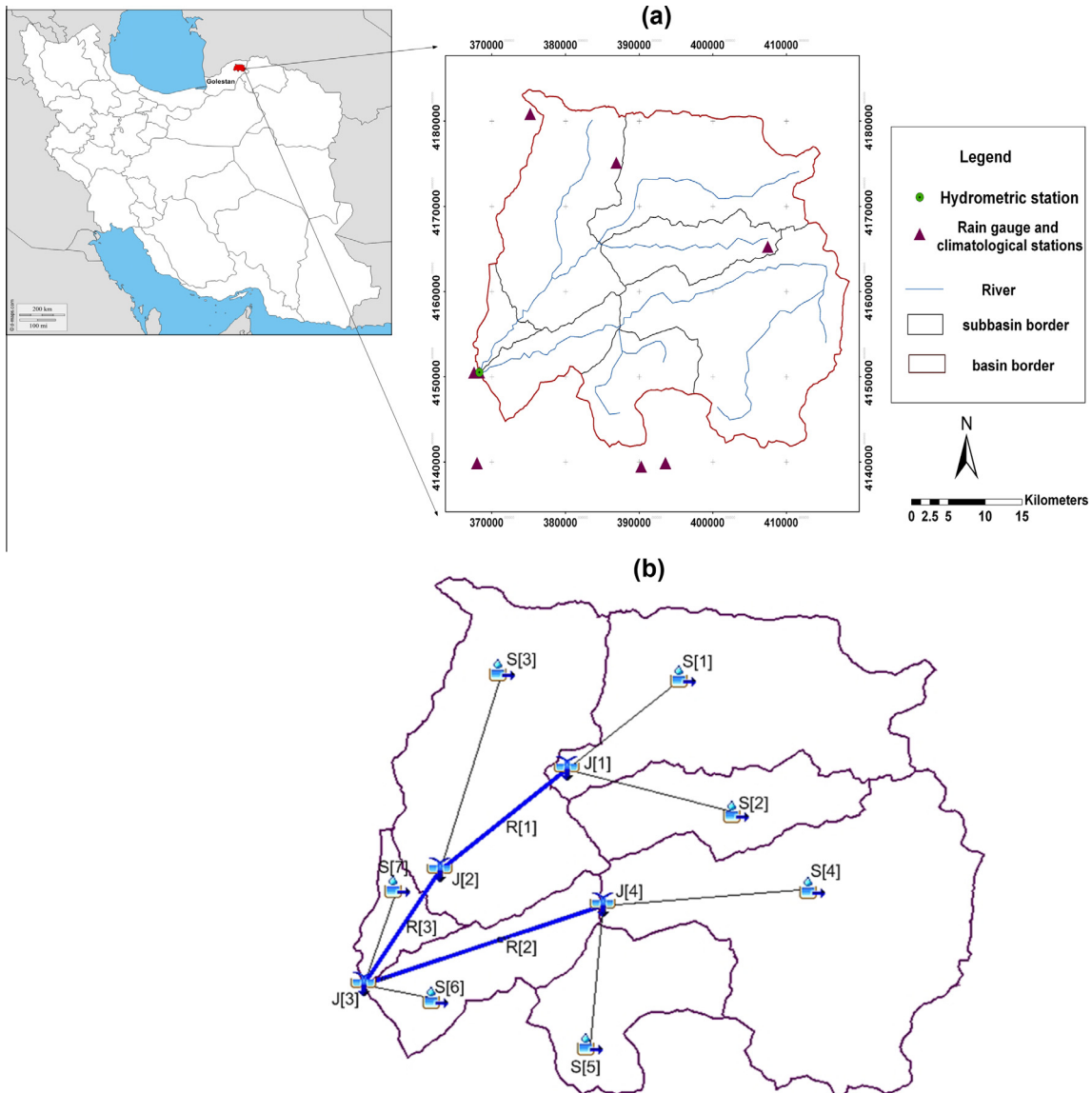


**Fig. 1.** (a) Study area and the sub-basins. (b) Schematic representation of Tamar basin model in HEC-HMS.

highest point. In this area, the dominant land use is pasture lands (approximately 39%). Close to 37% of the total area is covered by farmlands, and about 23% are forests. The rest of the area is barren land and urban areas.

There is only one hydrometric station which is located at the basin outlet (junction 3) with reliable records of discharge data. For each sub-basin, mean areal rainfall was calculated for each rainfall-runoff event through Thiessen method (Fig. 1a, Table 1). After screening all available data, four flood events were selected for further analysis (Table 2). Soil texture, land use, and soil hydrologic groups maps of the basin were provided from Natural Resources and Watershed Management Administration of Golestan (2007).

## 2.2. HEC-HMS hydrologic model

HEC-HMS software (USACE, 2013) was developed by Hydrologic Engineering Center (HEC) of US Army Corps of Engineers as a new version for HEC-1, which is commonly used for hydrologic simulations. Calibration and validation of parameters of the model can be conducted in HEC-HMS, so basin can be modeled by defining some

**Table 1**  
General information of meteorological and hydrometric stations.

Station	Coordinate of stations			Station type
	Longitude (UTM)	Latitude (UTM)	Elevation (m)	
Tamar	367,584	4,150,504	132	Hydrometeorology
Golidagh	407,429	4,165,341	1000	Rain gauge
Ghavijigh	375,224	4,180,871	500	Rain gauge
Gharnagh	386,892	4,175,154	500	Rain gauge
Ghochmaz	367,997	4,139,898	160	Rain gauge
Tangrah	390,288	4,139,471	330	Rain gauge
Golestan national park	393,568	4,139,903	460	Hydrometeorology
Tamar	367,911	4,149,683	132	Hydrometry

scenarios. In order to implement the HEC-HMS model, four elements should be followed, including meteorological model, basin model, time series data, and control specifications. Other necessary information may be classified as basin area, average curve number for sub-basins, initial abstractions, time of concentrations, routing characteristics, and base flow separation method. Next step is to

**Table 2**

Characteristics of selected flood events in Tamar basin.

Event	Date	Period	Peak flow (m <sup>3</sup> /s)	Duration (h)
1	19 September, 2004	Calibration	128	20
2	6 May, 2005	Calibration	299	30
3	9 August, 2005	Calibration	783	19
4	8 October, 2005	Validation	120	13

implement flood hydrographs and rainfall hyetographs in meteorological model, though the time period and time step of the simulation are requisite for control specifications. Soil Conservation Service-Curve Number (SCS-CN) and Clark methods were adopted for estimating hydrologic losses and transforming rainfall to runoff, respectively. Muskingum method was used for flow routing in the reaches. For flood events, base flow may not be significant. In this study, base flow was not considered since it has insignificant effect on the flood events (Mousavi et al., 2012; Kamali et al., 2013).

Curve number (CN) and initial abstraction ( $I_a$ ) are two parameters in SCS-CN method,  $I_a$  is expressed as follows:

$$I_a = aS \quad (1)$$

$$S = \frac{25,400 - 254CN}{CN} \quad (2)$$

where  $S$  is the maximum potential of soil moisture retention of the basin (mm), CN is the average curve number of basin,  $I_a$  is the initial abstraction (mm), and  $a$  is a coefficient equal to 0.2 (SCS, 1972), although various studies have reported different values (i.e., a range of 0–0.45) (Aron et al., 1997; Xiao et al., 2011; Gao et al., 2012; Mousavi et al., 2012; Kamali et al., 2013). This coefficient is different in various storms or basins (Baltas et al., 2007). In this study the initial range of  $a$  is considered to be between 0.035 and 0.45. Then the weighted average curve number of the sub-basins, as the initial curve number, was obtained by overlaying land use and hydrologic soil group maps and using standard CN tables. In the present study, antecedent moisture conditions of all three events (Table 2) were considered as the average condition.

Clark unit hydrograph method has two parameters, including time of concentration ( $T_c$ ), and storage coefficient ( $R$ ). The following equation can be used for calculating  $T_c$ , according to the SCS synthetic unit hydrograph method (Chow et al., 1988):

$$T_c = 1.67 \times \frac{(L \times 3.28)^{0.8} \times \left(\frac{1000}{CN} - 9\right)^{0.7}}{1900y^{0.5}} \quad (3)$$

where  $L$  is the length of the main channel (m),  $y$  is the slope of basin (%), CN is the average curve number of basin, and  $T_c$  is the time of concentration (h).

Storage coefficient and time of concentration are related as described by (Straub et al., 2000):

$$Cs = \frac{R}{R + T_c} \quad (4)$$

Two parameters of Muskingum routing method are  $Xm$  and  $km$  that can be estimated using cross section data given by Chow et al. (1988):

$$km = \frac{L}{3600 \cdot Cr} \quad (5)$$

$$Xm = \frac{1}{2} \left( 1 - \frac{Q}{B \cdot S \cdot Cr \cdot L} \right) \quad (6)$$

where  $Q$  is the discharge (CMS),  $Cr$  is the flood wave velocity (m/s),  $L$  is the channel length (m),  $B$  is the top width of flood area (m), and  $S$  is the bed slope (m/m) (USACE, 2000; IWRI, 2008).

### 2.3. Likelihood functions

Likelihood function represents the ability of HEC-HMS hydrologic model to exactly fit the observed data. Performance of each set of parameters in predicting the observed model may be evaluated by a likelihood measure (He et al., 2010). In order to assess the uncertainty of HEC-HMS, four informal likelihood functions (L1–L4) and three formal likelihood functions (L5–L7) were considered to evaluate their impacts on simulation results of DREAM<sub>(zs)</sub> method.

The first four likelihood functions, L1–L4, are Nash–Sutcliffe efficiency (NS; Nash and Sutcliffe, 1970), Normalized Absolute Error (NAE; Smith et al., 2008), Index of Agreement (IOA; Willmott et al., 1985), and Chiew and McMahon, respectively (CM; Chiew and McMahon, 1994). In the majority of the hydrologic studies, Nash–Sutcliffe (NS) function is frequently used with GLUE method as a likelihood function (McMichael et al., 2006; Jin et al., 2010; Li et al., 2010). L5 is the same maximum likelihood function which was used by Makowski et al. (2002) and demonstrates the relationship between standard least squares fitting and Bayesian inference (Vrugt and Sadegh, 2013). Likelihood function L6 is a Heteroscedastic Maximum Likelihood Error (HMLE) estimator (Duan, 1991). Likelihood function L7 is a first-order autoregressive scheme of the error residuals that explicitly accounts for the autocorrelation of residuals.

#### 2.3.1. Informal likelihood functions

Four informal likelihood functions, L1–L4, namely NS efficiency (17), Index of agreement (IOA; Eq. (8)), Normalized absolute error (NAE; Eq. (9)), and CM (Eq. (10)) are described as:

$$L_1(\theta_i|O) = NS = 1 - \frac{\sigma_e^2}{\sigma_o^2} = 1 - \frac{\sum_{j=1}^M (P_j(\theta_i) - O_j)^2}{\sum_{j=1}^M (O_j - \bar{O})^2} \quad (7)$$

$$L_2(\theta_i|O) = IOA = 1 - \frac{\sum_{j=1}^M (P_j(\theta_i) - O_j)^2}{\sum_{j=1}^M (|P_j(\theta_i) - \bar{O}| + |O_j - \bar{O}|)^2} \quad (8)$$

$$L_3(\theta_i|O) = NAE = 1 - \frac{\sum_{j=1}^M |P_j(\theta_i) - O_j|}{\sum_{j=1}^M |O_j - \bar{O}|} \quad (9)$$

$$L_4(\theta_i|O) = CM = 1 - \frac{\sum_{j=1}^M (P_j(\theta_i)^{\frac{1}{2}} - O_j^{\frac{1}{2}})^2}{\sum_{j=1}^M (O_j^{\frac{1}{2}} - \bar{O}^{\frac{1}{2}})^2} \quad (10)$$

where  $i = 1, 2, 3, \dots, N$  in all of the equations,  $\theta_i$  is the  $i$ th set of parameters,  $P_j(\theta_i)$  is the  $j$ th type of model output (simulated stream flow) under  $\theta_i$  set of parameters,  $O$  is the observed stream flow,  $O_j$  is the  $j$ th observation of  $O$ ,  $\bar{O}$  is the mean value of observations (Eq. (11)),  $N$  is the number of parameter sets, and  $M$  is the number of observations.

$$\bar{O} = \frac{1}{M} \sum_{j=1}^M O_j \quad (11)$$

#### 2.3.2. Formal likelihood functions

2.3.2.1. Homoscedastic (stationary) error case. Vector of residuals may be specified by the difference between  $P(\theta)$  and  $O$ .

$$\varepsilon_j(\theta) = P_j(\theta) - O_j \quad j = 1, 2, 3, \dots, M \quad (12)$$

The closer the residuals to zero, the better the model simulation matches measured data. However, residuals never become zero, due to input (rainfall) errors, model structural errors, errors in output measurements  $O_j$ , and uncertainties associated with the values

of parameter. Better correspondence between model predictions and observations is usually obtained by tuning the values of parameters and applying inference methodology that considers all sources of error separately (Vrugt et al., 2008).

If error residuals (Eq. (12)) are assumed to be independent (uncorrelated) and Gaussian-distributed with a constant variance  $\sigma^2$  and a zero mean, likelihood function L5 (Eq. (13)) is defined as:

$$L_5(\theta_i|O) = \prod_{j=1}^M \frac{1}{\sqrt{2\pi\sigma^2}} \exp\left(-\frac{(P_j(\theta_i) - O_j)^2}{2\sigma^2}\right) \quad (13)$$

where  $\sigma^2$  is the variance of errors of the model.

$$\sigma^2 = \frac{\sum_{j=1}^M (P_j(\theta) - O_j)^2}{M} \quad (14)$$

The logarithm of the likelihood function (or log-likelihood function) is conveniently used rather than the likelihood function (Eq. (13)), due to algebraic simplicity and numerical stability; the log-likelihood of Eq. (13) is:

$$l_5(\theta_i|O) = -\frac{M}{2} \ln(2\pi) - \frac{M}{2} \ln\sigma^2 - \frac{1}{2} \sigma^{-2} \times \sum_{j=1}^M \varepsilon_j(\theta_i)^2 \quad (15)$$

When homoscedasticity (stationarity) assumption of residuals is violated, a Box–Cox transformation (Box and Cox, 1964) of the simulated and measured streamflow data with parameter  $\lambda$  is used to induce homoscedasticity (constant variance) and remove skewness:

$$O^* = \begin{cases} \frac{(O^{\lambda}-1)}{\lambda} & \text{if } \lambda \neq 0 \\ \ln(\lambda) & \text{if } \lambda = 0 \end{cases} \quad (16)$$

$$P^*(\theta) = \begin{cases} \frac{(P(\theta)^{\lambda}-1)}{\lambda} & \text{if } \lambda \neq 0 \\ \ln(\lambda) & \text{if } \lambda = 0 \end{cases} \quad (17)$$

where  $O^*$  and  $P(\theta)^*$  are the transformed data, and  $\lambda$  is the transformation parameter.

**2.3.2.2. Heteroscedastic error case.** The HMLE estimator is the heteroscedastic maximum likelihood error (HMLE) estimator under the assumptions that error residuals are Gaussian-distributed with a zero mean, uncorrelated and heteroscedastic (non-homogeneous variance). In Heteroscedastic error case, variance of errors increases as a function of streamflow discharge (Sorooshian and Dracup, 1980). The HMLE estimator is described as (Sorooshian and Gupta, 1983):

$$HMLE = \frac{-\sum_{j=1}^M w_j \varepsilon_j(\theta_i)^2}{M \times \left(\prod_{j=1}^M w_j\right)^{\frac{1}{M}}} \quad (18)$$

where  $w_j$  is the weight assigned to the time  $j$ , and is given by:

$$w_j = f_j^{2(\lambda-1)} \quad (19)$$

where expected  $f_j$  can be approximated by either  $O_j$  or  $P_j(\theta)$  and  $\lambda$  is an unknown transformation parameter that stabilizes the variance. In this study a  $f_j$  equal to  $O_j$  was used to compute the weight (Sorooshian et al., 1993; Freedman et al., 1998). Duan (1991) developed a stable procedure for estimating  $\lambda$  where the HMLE estimator is computed by:

$$L_6(\theta_i|O) = HMLE = \frac{-R_n}{M \times \exp(2(\lambda-1)a_d)} \quad (20)$$

where

$$R_n = \sum_{j=1}^M w_j (P_j(\theta) - O_j)^2 a_j \quad (21)$$

$$a_j = \frac{\ln O_j}{a_d} \quad (22)$$

$a_d$  is the logarithmic average of the observed stream flow and is computed as:

$$a_d = \frac{1}{M} \sum_{j=1}^M \ln O_j \quad (23)$$

An iterative procedure is then followed to estimate  $\lambda$  such that  $R = 0$  in the following equation:

$$R = \frac{R_n}{R_d} - 1 \quad (24)$$

After running rainfall-runoff model by DREAM<sub>(ZS)</sub> algorithm under the formal likelihood function L5, assumptions of the residual error were evaluated.

The HMLE estimator was applied as the likelihood function (L6) to estimate the transformation parameter  $\lambda$  and testing homoscedastic assumption of residual errors of the study. Note that when error residuals are homoscedastic (constant variance), the value of  $\lambda$  is close to 1. On the other hand, for heteroscedastic error cases, the value of  $\lambda$  is near to 0 (Duan, 1991).

Kolmogorov–Smirnov test (Massey, 1951) was employed to evaluate the normality assumption of residual errors.

Durbin–Watson ‘d’ statistic test (Durbin and Watson, 1971) also was used as a test for detecting correlated errors (Sorooshian and Dracup, 1980).

**2.3.2.3. Correlated error case.** In the hydrologic modeling, the assumption of independent errors is not realistic and the errors are usually autocorrelated due to the uncertainty of the observed data and structural inadequacy of model. Therefore, a first-order autoregressive (AR) scheme of the residuals was applied to account for the correlated errors. A first-order autoregressive (AR – 1) scheme of the residuals removes the autocorrelation of the residuals. AR – 1 model is incorporated into the formulation of the log-likelihood function as follows (Sorooshian and Dracup, 1980; Vrugt et al., 2009b; Wöhling and Vrugt, 2011):

$$L_7(\theta_i|O) = -\frac{M}{2} \ln(2\pi) - \frac{1}{2} \ln \frac{\sigma_v^{2M}}{1-\rho^2} - \frac{1}{2} (1-\rho^2) \times \sigma_v^{-2} \varepsilon_1^*(\theta_i)^2 - \frac{1}{2} \sigma_v^{-2} \times \sum_{j=2}^M \delta_j(\theta_i, \rho)^2 \quad (25)$$

where  $\sigma_v^2$ s are the variance of model errors (Eq. (30)),  $\rho$  is the first-order autocorrelation coefficient,  $\delta_j(\theta, \rho)$  is the AR – 1 corrected time series of residuals (Eq. (29)) and  $\varepsilon^*(\theta)$  is the vector of residuals after Box–Cox transformation (Eq. (27)). Note that for  $\rho = 0$  and untransformed residuals (no Box–Cox transformation), Eq. (25) is reduced to Eq. (15). The likelihood function should be changed for estimating  $\lambda$  (Bates and Campbell, 2001; Yang et al., 2007a,b):

$$L_7(\theta_i|O) = L_7(\theta_i|O) + (\lambda - 1) \sum_{j=1}^M \ln(O_j) \quad (26)$$

where  $\varepsilon^*(\theta)$  is the vector of the transformed residuals, therefore is given by:

$$\varepsilon_j^*(\theta) = P_j^*(\theta) - O_j^* \quad j = 1, 2, 3, \dots, M \quad (27)$$

A first-order autoregressive (AR – 1) scheme of the transformed residuals is given by:

$$\varepsilon_j^* = \rho \varepsilon_{j-1}^* + \delta_j \quad j = 1, 2, 3, \dots, M \quad (28)$$

where  $\delta \sim N(0, \sigma_\delta^2)$  is the residual error with a zero mean and a constant variance  $\sigma_\delta^2$ . Adjusted AR – 1 time series of residuals is based on the following equation:

$$\delta_j(\theta, \rho) = \varepsilon_j^*(\theta) - \rho \varepsilon_{j-1}^*(\theta) \quad j = 1, 2, 3, \dots M \quad (29)$$

where  $\varepsilon_i \sim N\left(0, \frac{(\sigma_\nu^2)_i}{(1-(\rho^2)_i)}\right)$  is the residual error.  $\sigma_\nu^2$  is computed by multiplying the outcome of the following equation by  $\frac{M}{z}$  where  $z$  is drawn from a chi-squared distribution with  $M$  degrees of freedom (Vrugt et al., 2009b; Laloy et al., 2010).

$$(\sigma_\nu^2)_i = \frac{M}{z} s^2 \quad (30)$$

where  $s^2$  is described by:

$$s^2 = \frac{1}{M} ((\varepsilon_1^*)^2 (1 - \rho^2) + \sum_{j=2}^M \delta_j^2) \quad (31)$$

The transformation parameter ( $\lambda$ ) and the first-order correlation coefficient ( $\rho$ ) are estimated together with the parameters of the hydrologic model (Table 3) during the calibration. Prior uncertainty ranges of the first-order correlation coefficient ( $\rho$ ) and the transformation parameter ( $\lambda$ ) are considered to be between 0 and 1 (Laloy et al., 2010; Schoups and Vrugt, 2010).

In this approach, the number of parameters that needs to be estimated is increased significantly. Therefore, DREAM<sub>(zs)</sub> method, which is based on Markov chain Monte Carlo (MCMC) sampler, is used to estimate the high-dimensional posterior distributions efficiently.

#### 2.4. Parameter uncertainty

The analysis is based on a nonlinear regression model, according to the following equation:

$$Y = E + \varepsilon \quad (32)$$

where  $Y$  is the vector of observations;  $E$  is the vector of expected values which corresponds to  $Y$ ; and  $\varepsilon$  is the vector of random errors or residuals, which includes three types of errors (i.e. output measurements, input (rainfall) errors, and model structural errors).

Residual errors are defined by a joint probability density function (pdf) and a vector of its parameters ( $\theta_\varepsilon$ ). A common approach is to assume that the errors are independent (uncorrelated) and Gaussian-distributed with a zero mean and a constant variance,  $N(0, \sigma^2)$  (Schoups and Vrugt, 2010). Parameter uncertainty for the given observed data  $Y$ , may be expressed by posterior probability density functions of parameters (Box and Tiao, 1992),

$$p(\theta|Y) \propto l(\theta|Y)p(\theta) \quad (33)$$

where  $\theta = \{\theta_\varepsilon, \theta_h\}$  is the vector of parameters, including parameters of hydrologic model,  $\theta_h$ , and those of residual error model  $\theta_\varepsilon$ ,  $p(\theta)$  is the prior probability density functions of parameters, and  $l(\theta|Y)$  is the likelihood function.

**Table 3**

The lower and upper bounds for calibration parameters.

Parameter	Location	Lower limit	Upper limit
Curve number (CN)	Sub-basin-1 <sup>a</sup> (S1)	65	89
	Sub-basin-2 (S2)	68	93
	Sub-basin-3 (S3)	68	93
	Sub-basin-4 (S4)	66	90
	Sub-basin-5 (S5)	64	87
	Sub-basin-6 (S6)	69	93
	Sub-basin-7 (S7)	71	96
Loss coefficient (a)	7 Sub-basins	0.035	0.45
Regional value (Cs)	7 Sub-basins	0.2	0.65
Muskingum routing (Xm)	3 Reaches	0.2	0.5

<sup>a</sup> For definition of sub-basins, see Fig. 1.

Once the prior probability density functions of parameters are specified, likelihood function can be applied to define the uncertainty of posterior parameter using repeated Monte Carlo sampling of the sets of parameters from prior parameter space (e.g. by Monte Carlo Markov chain-MCMC-samplers). In order to estimate the uncertainty of parameters, after convergence is reached, the last 20% of posterior parameter sets of the model were used to produce model outputs. The Gelman-Rubin diagnostic is used to check the convergence. Results were then analyzed and 95% confidence interval was drawn by calculating 2.5% and 97.5% percentiles.

#### 2.5. Total predictive uncertainty

In order to estimate the total predictive uncertainty, the residual errors is expected to be additive. In informal likelihood functions and likelihood function L6, it was assumed that the residual errors are Gaussian-distributed with a zero mean and a constant variance. For each individual model prediction from the last 20% of the samples, which were generated after convergence to the posterior distribution, the residual error,  $\varepsilon_i \sim N(0, \sigma^2)$  was added to the model prediction  $P(\theta_i)$ . Then the corresponding results were used to obtain the 95% total prediction uncertainty bounds including parameter, model structure and measurement errors by computing 97.5% and 2.5% prediction percentiles.

In the HMLE estimator, errors are assumed to be Gaussian, uncorrelated and heteroscedastic (non-homogeneous variance)  $(0, \sigma_j^2)$ .

Variance of the untransformed flows ( $\sigma_j^2$ ) may be characterized based on Bartlett's (1947) method by the following equation (Sorooshian and Dracup, 1980):

$$\sigma_j^2 \approx f_j^{2(1-\lambda)} \sigma^2 \quad (34)$$

where  $f_j = O_j$  was used in this study (Sorooshian et al., 1993; Freedman et al., 1998),  $\lambda$  is an unknown transformation parameter that stabilizes the variance, and  $\sigma^2$  is the constant variance of the transformed flow. For each individual model prediction  $P(\theta_i)$  and posterior parameter  $\lambda_i$  from the last 20% of the samples, which were generated after convergence to the posterior distribution, the residual error  $\varepsilon_i \sim N(0, \sigma_j^2)$  was added to model prediction  $P(\theta_i)$ . The results were used to compute 97.5% and 2.5% prediction percentiles.

For likelihood function L7 (correlated error case), Vrugt et al. (2009b) proposed the following equation to determine the residual error:

$$\varepsilon_i \sim N\left(0, \frac{(\sigma_\nu^2)_i}{(1-(\rho^2)_i)}\right) \quad (35)$$

For each individual model prediction  $P(\theta_i)$  and posterior parameters including transformation parameter  $\lambda_i$  and first-order correlation coefficient ( $\rho_i$ ) from the last 20% of the samples, which were generated after convergence to the posterior distribution, the residual error  $\varepsilon_i$  was added to each model prediction in the transformed output space  $P^*(\theta_i)$ :

$$Z^* = P^*(\theta_i) + \varepsilon_i \quad (36)$$

After back transforming  $Z^*$  output to the original output space, a 95% total predictive uncertainty interval can again be obtained by calculating the 2.5% and 97.5% percentiles.

#### 2.6. Markov chain Monte Carlo sampling with DREAM<sub>(zs)</sub>

DREAM<sub>(zs)</sub> algorithm is taken from Markov chain Monte Carlo (MCMC) sampler and is based on the original DREAM algorithm (Differential Evolution Adaptive Metropolis algorithm) but it is modified for using samples from an archive of past states to gener-

ate candidate points in each individual chain. Details of DREAM algorithm are described in other studies (Vrugt et al., 2009a,b) so, they will not be considered in this study.

This algorithm was designed to speed up convergence to the posterior distribution for complex, multimodal, and high-dimensional search problems. DREAM<sub>(ZS)</sub> uses only three parallel chains to appropriately estimate the posterior probability density function, by which convergence to the posterior distribution is accelerated. DREAM<sub>(ZS)</sub> includes a snooker updater to generate jumps beyond parallel direction updates (ter Braak and Vrugt, 2008) which increases diversity of candidate points. Schoups and Vrugt (2010) used DREAM<sub>(ZS)</sub> algorithm to estimate the uncertainty of parameter and prediction in the context of hydrologic modeling. In this study Latin hypercube sampling was used to draw an initial population of parameters. In order to diagnose convergence of the chain to the posterior distribution, R-statistic of Gelman-Rubin (Gelman and Rubin, 1992) was adopted to monitor the convergence.

Once convergence criterion was satisfied less than 1.2 for all parameters, algorithm is said to be converged to the posterior target distribution (Vrugt et al., 2009a,b). Posterior probability distributions of parameters of the rainfall-runoff model are formed using the last 20% of samples generated with DREAM<sub>(ZS)</sub>, once they are converged to posterior distribution in the calibration period.

For representing parameter sensitivity to the choice of likelihood functions, cumulative distributions of the last 20% of parameters after convergence, which were used in validation phase, were obtained for seven likelihood functions.

The two-sample Kolmogorov-Smirnov test (Massey, 1951) was applied to evaluate the difference between cdfs of the posterior distributions (the last 20% of parameters after convergence) and the uniform prior distributions of parameters for different likelihood functions. Therefore, uniform prior distributions of parameters were generated using prior ranges (Table 3).

The difference between the cdfs of the posterior distributions and the cdf of the uniform prior distribution for each parameter under seven likelihood functions can be estimated using statistics of Kolmogorov-Smirnov test ( $D$ ) according to the following equation:

$$D = \max(|F_1(x) - F_2(x)|) \quad (37)$$

where  $F_1(x)$  and  $F_2(x)$  are cdf of the posterior distributions and prior distributions of parameters.

The higher  $D$  shows that posterior distributions of parameters are more different from the uniform prior distribution and the corresponding parameter is more sensitive and is associated with less uncertainty. The cumulative distribution of a uniform distribution is a straight line (approximately a 1:1 slope). Deviations from this straight line indicate higher identifiability of parameters (Wagener et al., 2002; Abebe et al., 2010).

## 2.7. Ranges of sampling parameters

In this study, curve number (CN), loss coefficient ( $a$ ), regional value ( $C_s$ ) (Eq. (4)) and routing parameter ( $X_m$ ) were considered as the calibration parameters, and prior uncertainty ranges of these parameters were used in DREAM<sub>(ZS)</sub> uncertainty algorithm. For the curve number, ±15 percent of the initial values were taken as the upper and lower bounds of CN. There are three calibration parameters for each sub-basin, including curve number (CN1–CN7), loss coefficient ( $a_1$ – $a_7$ ), and regional value ( $C_s1$ – $C_s7$ ), which result in a total of 21 parameters. There are also three routing parameters  $-X_m$  (one for each reach), therefore, total number of calibration parameters would be equal to 24. Assuming uniform priors for all parameters, the upper and lower bounds (prior uncertainty

ranges) of all the parameters of hydrologic model in each sub-basin are listed in Table 3.

After importing data and parameters of DREAM<sub>(ZS)</sub> algorithm and rainfall-runoff model, DREAM<sub>(ZS)</sub> algorithm was linked to HEC-HMS model in MATLAB software, and then HEC-HMSmodel was run. The first three events were used for calibration and the last one was taken to account for validation (Table 2).

## 2.8. Performance assessment criteria for DREAM<sub>(ZS)</sub> and different likelihood functions

In this study the employed indicators of uncertainty assessment are P-factors (percentage of measured data bracketed by 95% prediction uncertainty, 95PPU) (Vrugt et al., 2009b; Li et al., 2010; Abbaspour, 2011; Alazzy et al., 2015), and R-factors (average thickness of 95PPU band divided by standard deviation of measured data) (Abbaspour, 2011). Once most of the measured data are bracketed with the smallest possible R-factor, a better performance of DREAM<sub>(ZS)</sub> algorithm is fulfilled.

After running rainfall-runoff model with DREAM<sub>(ZS)</sub> algorithm for each flood event, simulated flow obtained from the best set of parameters (with maximum likelihood function or minimum objective function) will be compared with observed flows. Statistical indicators including root-mean-square error (RMSE, Eq. (38)), Kling-Gupta Efficiency (KGE, Eq. (39)) (Gupta et al., 2009), and Nash-Sutcliffe (NS, Eq. (40)) criteria were used to compare the performance of DREAM<sub>(ZS)</sub>.

$$\text{RMSE} = \sqrt{\frac{\sum_{i=1}^n (y_{\text{esti}} - y_{\text{acti}})^2}{n}} \quad (38)$$

$$\text{KGE} = 1 - \sqrt{(cc - 1)^2 + (\alpha - 1)^2 + (\beta - 1)^2} \quad (39)$$

$$\text{NS} = 1 - \frac{\sum_{i=1}^n (y_{\text{esti}} - y_{\text{acti}})^2}{\sum_{i=1}^n (y_{\text{acti}} - \bar{y}_{\text{acti}})^2} \quad (40)$$

where  $y_{\text{acti}}$  is the observed discharge,  $\bar{y}_{\text{acti}}$  is the mean value of observations,  $y_{\text{esti}}$  is the simulated discharge,  $n$  is the number of observations,  $cc$  is the linear correlation coefficient between  $y_{\text{act}}$  and  $y_{\text{est}}$ ,  $\alpha$  is the ratio of standard deviation of  $y_{\text{est}}$  to standard deviation of  $y_{\text{act}}$ , and  $\beta$  is the ratio of the mean of  $y_{\text{est}}$  to mean of  $y_{\text{act}}$ . The smallest possible RMSE along with KGE and NS close to 1, represents a better performance of likelihood function.

## 3. Results and discussion

### 3.1. Evaluation of residual error assumptions

In likelihood function L5, residual errors are assumed to be independent (uncorrelated) and Gaussian-distributed with a constant variance  $\sigma^2$  and a zero mean. After running rainfall-runoff model with DREAM<sub>(ZS)</sub> algorithm under likelihood function L5 for each flood event, residual errors of simulated flow were evaluated which were obtained from the best set of parameters (the maximum-likelihood parameter set). The assumptions of the residual error for the first three events, which were used in the calibration period, can be visually assessed by using the graphs shown in Fig. 2. Kolmogorov-Smirnov test confirmed that the normality assumption is rejected for each flood event (Fig. 2a). Also, residual errors, as a function of simulated flow, do not show evident heteroscedasticity for each flood event (Fig. 2b).

By assuming that errors are heteroscedastic, HMLE estimator was applied as a likelihood function for estimating transformation parameter  $\lambda$ , Eq. 20. After running rainfall-runoff model with DREAM<sub>(ZS)</sub> algorithm and based on HMLE likelihood function, a

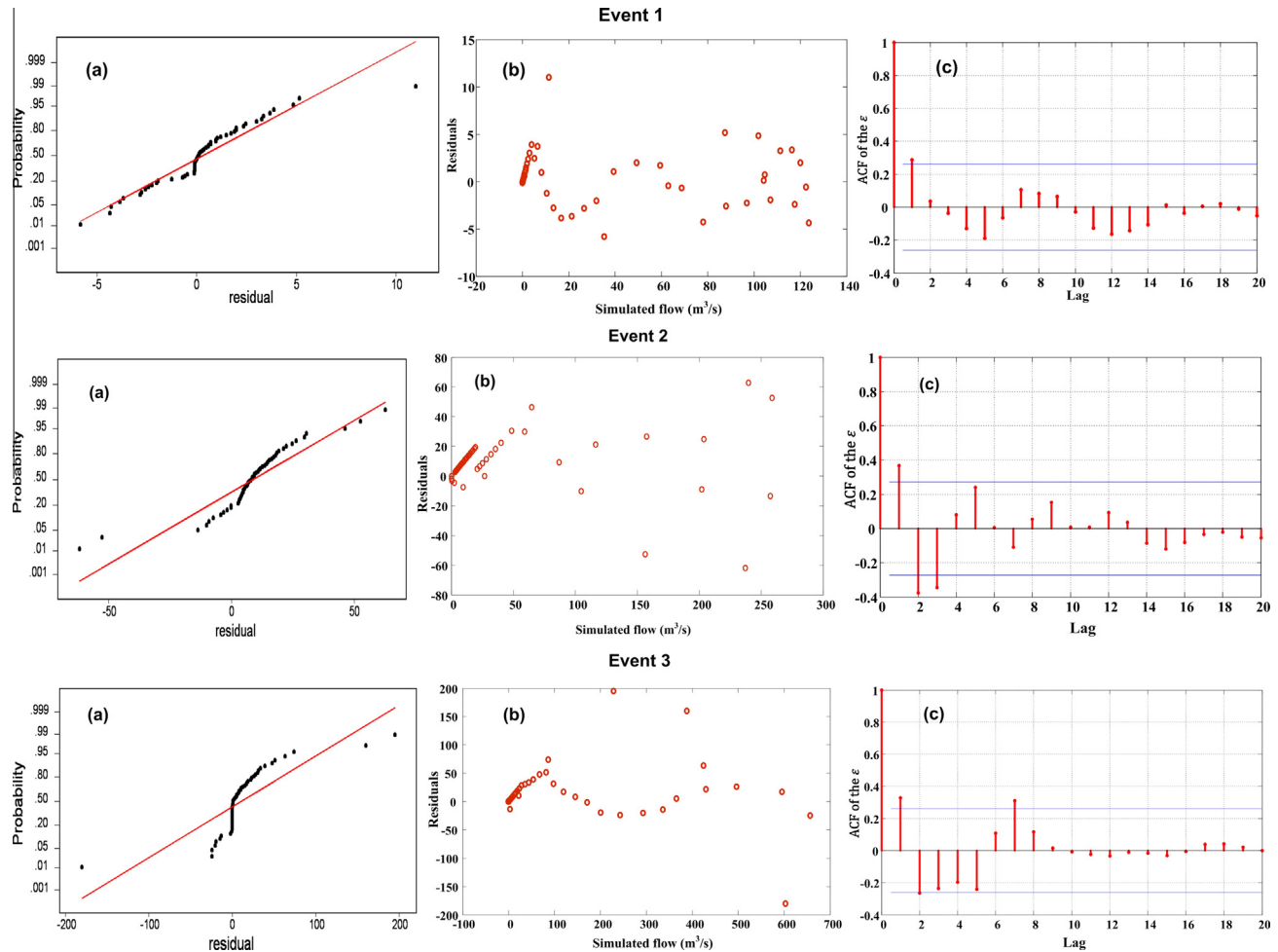


**Fig. 2.** Results of residual analysis for the first three flood events employed in the calibration period using the maximum likelihood parameter set under likelihood function L5: (a) Normal probability plot of residuals, (b) residuals as a function of simulated streamflow, and (c) autocorrelation function plot of residual series.

posterior histogram of the transformation parameter  $\lambda$  was identified, such that its highest probability density was approximately 0.65 (shown in the next section). The value of  $\lambda$  showed that residual errors are heteroscedastic.

In this study, the effectiveness of Durbin–Watson ‘*d*’ statistic test was also examined as a measure for detecting correlated errors. The ‘*d*’ statistic of this test showed that residuals are correlated. Another support was due to partial autocorrelation of residual series (Fig. 2c) which showed that errors are correlated at the first lag for each flood event (lag-1) (between 0.2 and 0.4).

A Box–Cox transformation of observed and simulated streamflows was used to account for relaxing the heteroscedasticity and skewness. A first-order autoregressive (AR) scheme of the residuals was then applied to cancel out the autocorrelation of the residuals and AR – 1 model was incorporated into the formulation of the log-likelihood function after Box–Cox transformation (likelihood function L7). Fig. 3 represents that temporal autocorrelation of residuals has been removed by using an AR1 model incorporated into the formulation of the log-likelihood function. Temporal autocorrelation of residuals is small at lag-1 in Fig. 3 compared to Fig. 2.

### 3.2. Posterior probability distributions of parameters

Based on Table 3, the total number of calibration parameters is equal to 24, including curve number (CN), loss coefficient ( $a$ ), regional value ( $C_s$ ), and routing parameter ( $X_m$ ). Calibration and

assessment of model uncertainty were done separately for each event, while event number 4 (Table 2) was used for validation.

In the validation phase, HEC-HMS model was run considering all the likelihood functions and using the last 20% of samples generated by DREAM<sub>(ZS)</sub>. In addition, the convergence to the posterior distribution is met in the calibration period. According to the results, for likelihood function L2, the posterior distributions of parameters of the third flood event (Table 2) were more sensitive and had less uncertainty. Posterior distributions of parameters of the second flood event (Table 2) and the first flood event (Table 2) were more sensitive and had less uncertainty for likelihood functions L1, L3, L4 and likelihood functions L5, L6, L7, respectively (not shown owing to the space limitation). Posterior distributions of parameters of these flood events were used for the validation phase.

Actually, posterior distribution of each parameter depends on the specifications of each event (Heidari et al., 2006; Dotto et al., 2011), and parameter distributions resulted from simulation of one single event are unique for each flood event (Pourreza-Bilondi et al., 2012). Although there may be some similarities between these distributions corresponding to events with similar characteristics (e.g. moisture conditions, peak discharge values, date of flood events).

Posterior histograms of the last 20% of parameters used in validation phase are presented in the next section (Fig. 6).

In order to represent the sensitivity of parameters to the choice of likelihood functions, after convergence, cumulative distributions

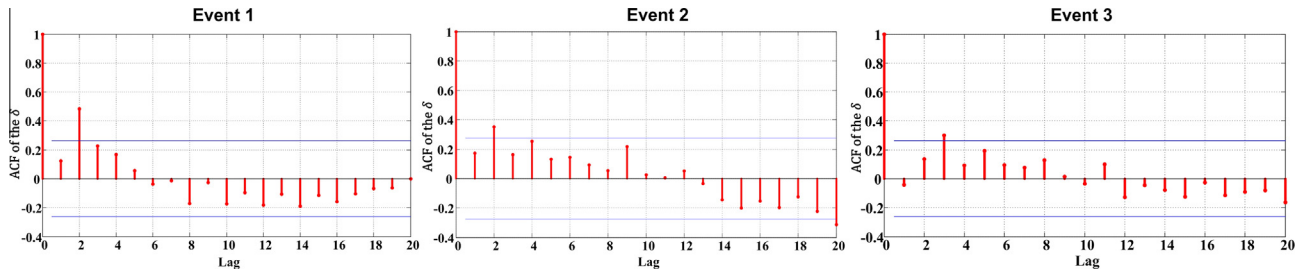


**Fig. 3.** Autocorrelation function plot of residual series after Box-Cox and AR1 transformation for first three flood events employed in the calibration period by using the maximum likelihood parameter set.

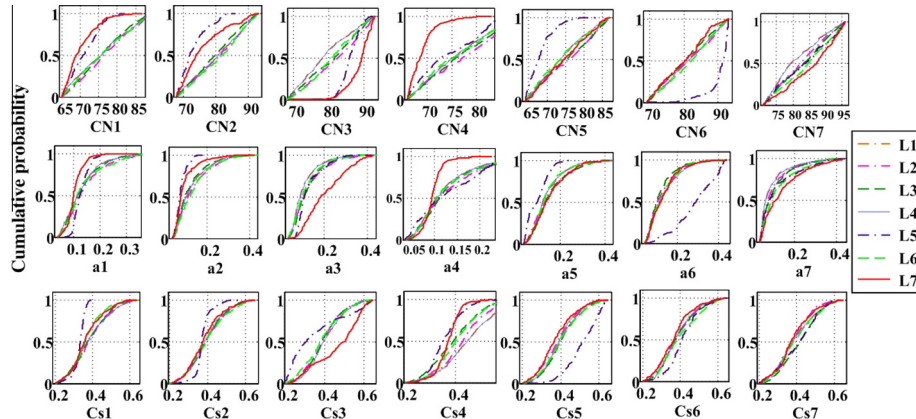


**Fig. 4.** Cumulative distribution functions of the last 20% of parameters used in validation phase for informal likelihood functions (L1–L4) and formal likelihood functions (L5–L7).

of the last 20% of parameters were obtained for seven likelihood functions in the validation phase (parameters of the third flood event for the likelihood function L2; parameters of the second flood event for the likelihood functions L1, L3, L4; and parameters of the first flood event for the likelihood functions L5, L6, L7).

Fig. 4 clearly shows that the likelihood function is strongly effective on sensitivity of parameters. Sensitivity is not the same for different likelihood functions. Therefore, one should be careful in choosing a likelihood function due to their importance to parameter values.

Importance of likelihood functions may be found in literature. Assessing the cumulative distributions of posterior parameters in Xinanjiang Rainfall-Runoff Model using GLUE method based on four different likelihood functions (NS, NAE, IOA and CM), Alazzy et al. (2015) showed that not all parameters have the same sensitivity to different likelihood functions. Abebe et al. (2010) showed that identifiability and sensitivity of parameters were quite different for the HBV hydrologic model with three objective functions (NS, RMSE and BIAS) in Leaf basin at Mississippi, USA.

Almost for most of the parameters, formal likelihood functions L5 and L7 (violet<sup>1</sup> dash line and red solid line) have completely different influence on sensitivity of parameters in comparison with the other likelihood functions. This result confirms Fig. 5 regarding Kolmogorov-Smirnov test statistic (D) applied to evaluate the difference between cdfs of the posterior distributions (the last 20% of parameters after convergence) and the uniform prior distributions of parameters for different likelihood functions.

Based on Fig. 4, almost for most of the parameters, the cumulative distributions of parameters of likelihood functions L5 and L7 have deviated more than other likelihood functions from straight

line (shape of cumulative distribution of a uniform prior). This result showed that most parameters are better defined by likelihood functions L5 and L7 and are more sensitive to the model performance. Therefore, they have less uncertainty and can be considered as easily identifiable parameters.

Comparing the cumulative distributions of different sets of parameter (CN1–CN7, a1–a7 and Cs1–Cs7) shows that (Fig. 4) the shape of cumulative distribution of different likelihood functions is unique for each parameter set. Moreover cumulative distributions corresponding to informal likelihood functions L1, L2, L3, L4 and formal likelihood function L6 are roughly equal for most of the sub-basins, and these likelihood functions have an almost similar effect on sensitivity of parameters. So, it may be concluded that parameters are not sensitive to the choice of these likelihood functions.

After running rainfall-runoff model coupled with DREAM<sub>(ZS)</sub> algorithm and with 7 different likelihood functions, 21 identifiable and sensitive parameters, out of 24 model parameters, were considered to obtain their posterior distributions. Routing parameters ( $Xm_1, Xm_2, Xm_3$ ) had uniform distribution and their posteriors did not change significantly in comparison with their prior distributions (not shown due to the space limitation), which presented a higher uncertainty.

Posterior histograms of the last 20% of parameters are presented in Fig. 6 which were used in validation phase of seven likelihood functions. Ranges and shapes of posterior distributions of parameters are very similar for informal likelihood functions L1, L2, L3 and L4. Posterior probability density functions obtained by informal likelihood functions (L1–L4) for most of the parameters (especially CN1–CN7) are wider and almost cover the entire uniform prior distributions (Table 3). Posterior distributions of CN1–CN7 obtained by informal likelihood functions L1–L4 and formal likelihood function L6 do not change significantly in comparison

<sup>1</sup> For interpretation of color in Fig. 4, the reader is referred to the web version of this article.

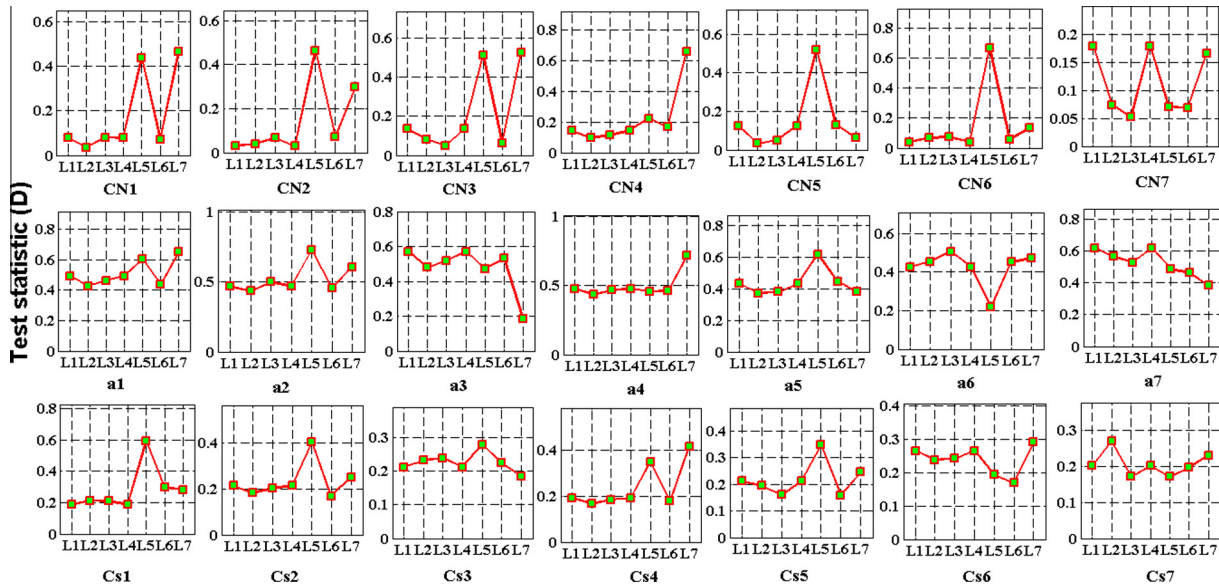


**Fig. 5.** Kolmogorov-Smirnov test statistic ( $D$ ) for the last 20% of parameters used in validation phase under seven different likelihood functions.

with their prior distributions, which presented a higher uncertainty.

The ranges and shapes of posterior distributions of the most of the parameters are different in two formal likelihood functions L5 and L7, as compared with the other formal and informal likelihood functions. Posterior distributions obtained by L5 and L7 were better defined for most of the parameters and resemble less uncertainty.

Among these functions, posterior distributions obtained by formal likelihood functions L5 and L7 are almost normal for most of the parameters, but the other ones tend to concentrate at their lower bounds. Width of posterior probability density functions were relatively small in L5 and L7, compared to uniform prior distributions (Table 3), which means that most of the parameters are better defined by L5 and L7. These parameters have less uncertainty and may be considered as easily identifiable parameters.

Vrugt et al. (2009b) and Schoups and Vrugt (2010) showed that the width or spread of the histograms of posterior parameter obtained by likelihood function L5 (based on assumptions inherent in SLS) and by likelihood function L7 (based on Box-Cox transformations and first-order autoregressive, AR – 1, scheme of the residuals) only covered a relatively small region for most of the parameters compared to uniform prior distributions, so these parameters had less uncertainty.

Based on Fig. 6b, posterior distribution of the first-order correlation coefficient parameter ( $\rho$ ) is approximately Gaussian with the highest probability density of approximately 0.2. This value of  $\rho$  confirms the presence of autocorrelation between the error residuals and highlights the need to use AR – 1 model incorporated into the formulation of the log-likelihood function.

On the other hand, highest probability density of posterior distribution of the transformation parameter  $\lambda$  is approximately 0.65 (Fig. 6b) that shows heteroscedasticity of residual errors and thus a Box-Cox transformation is needed for observed and simulated streamflow.

### 3.3. Coefficient of variation (CV) of parameters

In order to define levels (magnitude) of sensitivity of parameters, coefficient of variation (CV) is considered. Parameters with smaller CVs show that these parameters are more sensitive to the performance of model (He et al., 2010; Pourreza-Bilondi

et al., 2013; Shafiei et al., 2014; Alazzy et al., 2015). Fig. 7 and Table 4 show statistical characteristics (i.e. values of mean and coefficient of variation) of posterior parameter used for validation phase under different likelihood functions.

Based on Fig. 7, CV of the most of the parameters are smaller in formal likelihood functions L5 and L7, i.e. most parameters are better defined by L5 and L7 and are more sensitive to the performance of model. Therefore, they have less uncertainty and can be considered as easily identifiable parameters. This result confirms Fig. 6 regarding shapes of posterior distributions of these parameters.

In all the floods, smaller values of coefficient of variation (CV) for CN (less than 10%) show that posterior ranges overlap only a small part of the prior range, Fig. 7, therefore, this parameter is the most sensitive parameter to the model performance. Ponce and Hawkins (1996), Wang and Huang (2008), Kousari et al. (2010), Xiao et al. (2011), and Rafiee Sardoui et al. (2012) also found this result in their researches. CN plays an important role in maximum potential of soil moisture retention of the basin and subsequently runoff volume, so a careful estimation is required.

D-dimensional correlation matrix of posterior showed that under different likelihood functions there is a small linear correlation between parameters (not shown to be brief), thus observed data of the stream flow contain sufficient information to estimate these parameters. This point is supported by Vrugt et al. (2003, 2008).

Correlation coefficient of posterior parameter between CN and  $a$  was around 0.8 for all sub-basins and all flood events, suggesting that one of these parameters may be fixed in this basin before calibrating the hydrologic model. High correlation between parameters may also be found in literature. Schoups and Vrugt (2010) reported high correlation between maximum percolation rate and both evaporation and runoff in a lumped conceptual rainfall-runoff model (Schoups et al., 2010) based on FLEX modeling system (Fenicia et al., 2007). Vrugt et al. (2003) also found high correlation between spatial variability of soil moisture storage and maximum storage parameters in a watershed in the HYMOD conceptual rainfall-runoff model.

Based on the results of posterior distributions and coefficient of variation (CV) of parameters (Figs. 5–7), formal likelihood functions L5 and L7 have a relatively greater influence on the uncertainty analysis of parameter than the other likelihood functions which were accounted in this study.

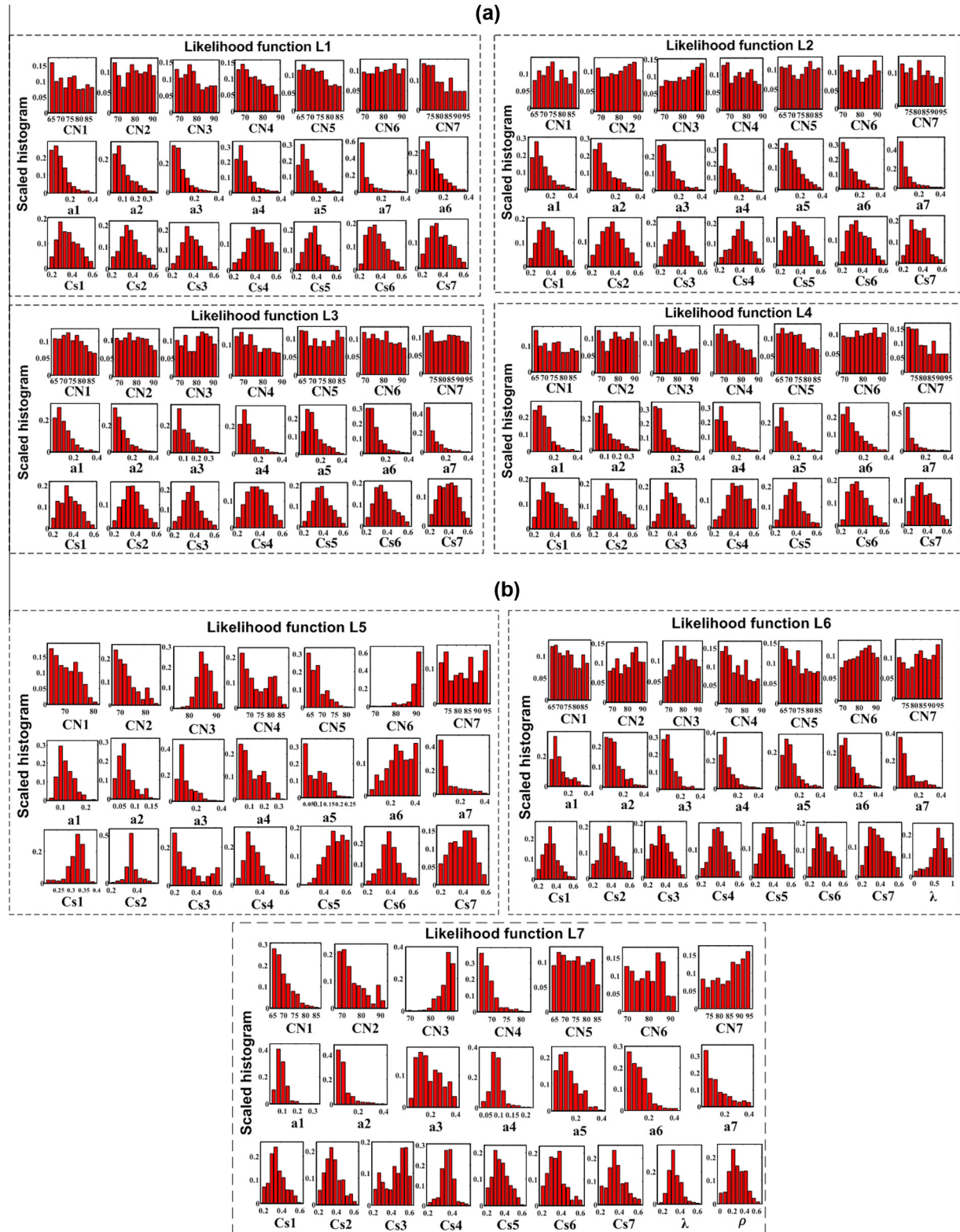


**Fig. 6.** (a) Posterior histograms of hydrologic model parameters using informal likelihood functions L1–L4 and (b) posterior histograms of hydrologic model parameters and transformation parameter  $\lambda$  and first-order correlation coefficient ( $\rho$ ) using formal likelihood functions L5–L7.

Based on the results, parameters derived from formal likelihood function L5 have less uncertainty and can be considered as easily identifiable parameters, although likelihood function L5 is highly depended on the assumptions of residual error (uncorrelated,

homoscedastic and normally distributed residuals). In this study, the assumptions of residual error were clearly violated (Fig. 2), therefore, likelihood function L5 may result in biased and unreliable estimation of the parameter. Thus, formal likelihood function

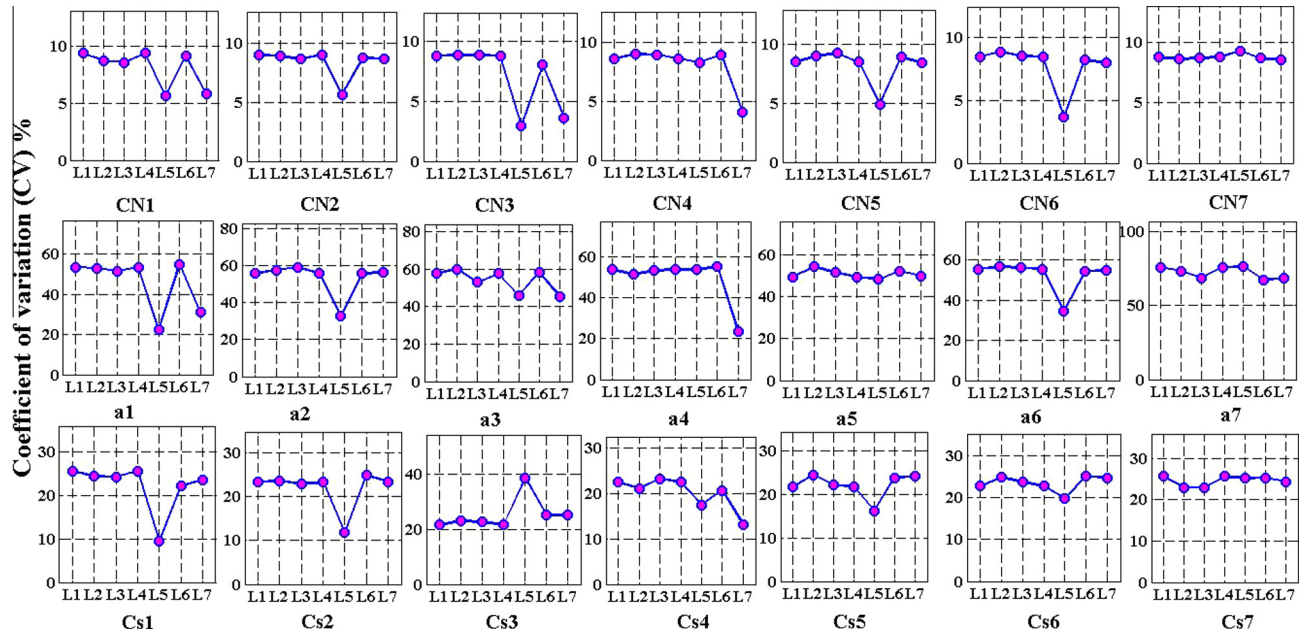


**Fig. 7.** Coefficient of variation of posterior distributions derived from different likelihood functions.

**Table 4**

Mean values of posterior distributions from application of DREAM<sub>(ZS)</sub> method with Likelihood Functions L1–L7.

Parameter	Likelihood						
	L1	L2	L3	L4	L5	L6	L7
CN1	75.81	76.82	75.93	75.81	71.05	76.11	70.08
CN2	80.57	80.77	79.91	80.57	73.20	81.26	76.12
CN3	79.06	81.91	80.84	79.06	86.02	80.97	88.60
CN4	76.05	77.21	76.67	76.05	74.32	76.01	69.07
CN5	74.18	75.66	75.30	74.18	68.26	74.11	74.90
CN6	81.22	81.03	80.28	81.22	90.33	81.61	80.00
CN7	81.18	82.61	83.12	81.18	83.54	84.24	85.60
a1	0.13	0.14	0.13	0.13	0.13	0.14	0.10
a2	0.13	0.14	0.12	0.13	0.08	0.14	0.10
a3	0.11	0.13	0.12	0.11	0.13	0.12	0.21
a4	0.12	0.13	0.13	0.12	0.13	0.13	0.10
a5	0.14	0.15	0.15	0.14	0.10	0.14	0.15
a6	0.13	0.13	0.12	0.13	0.28	0.13	0.13
a7	0.10	0.11	0.11	0.10	0.12	0.12	0.14
Cs1	0.38	0.39	0.38	0.38	0.33	0.37	0.37
Cs2	0.39	0.40	0.39	0.39	0.37	0.40	0.38
Cs3	0.40	0.39	0.39	0.40	0.35	0.39	0.46
Cs4	0.45	0.43	0.40	0.45	0.36	0.41	0.37
Cs5	0.40	0.39	0.41	0.40	0.51	0.40	0.38
Cs6	0.39	0.38	0.39	0.39	0.42	0.40	0.37
Cs7	0.39	0.38	0.42	0.39	0.41	0.40	0.38

L7 was used to relax common assumptions about residual errors that can provide reliable model parameters and therefore can be prescribed.

#### 3.4. Predicting uncertainty bounds of the model

Fig. 8 presents 95% prediction uncertainty bounds of HEC-HMS model estimated by DREAM<sub>(ZS)</sub> algorithm for 7 likelihood functions and each flood event. Based on Fig. 8, 95% total prediction uncertainty ranges may bracket most of the observed flows. By calculating uncertainty assessment indicator (*P*-factor), 95% total prediction uncertainty ranges covers 80–100% of observed data both in calibration and validation periods for different likelihood functions, but 95% total prediction uncertainty bounds are quite

wide (Fig. 8) which is an indication of considerable uncertainty in the model structure and measured input data.

For formal likelihood function L5, prediction uncertainty bounds do not contain observed peak flows for flood events 2 and 3. In addition, prediction uncertainty is overestimated for low flows and underestimated for peak flows due to the use of a constant error variance and ignoring heteroscedasticity (Fig. 8), as pointed out by Schoups and Vrugt (2010) and Koskela et al. (2012).

Assumptions of constant variance and normally distributed residuals are clearly violated in likelihood function L5, therefore, likelihood function L5 yields unrealistic prediction uncertainty bounds (Schoups and Vrugt, 2010).

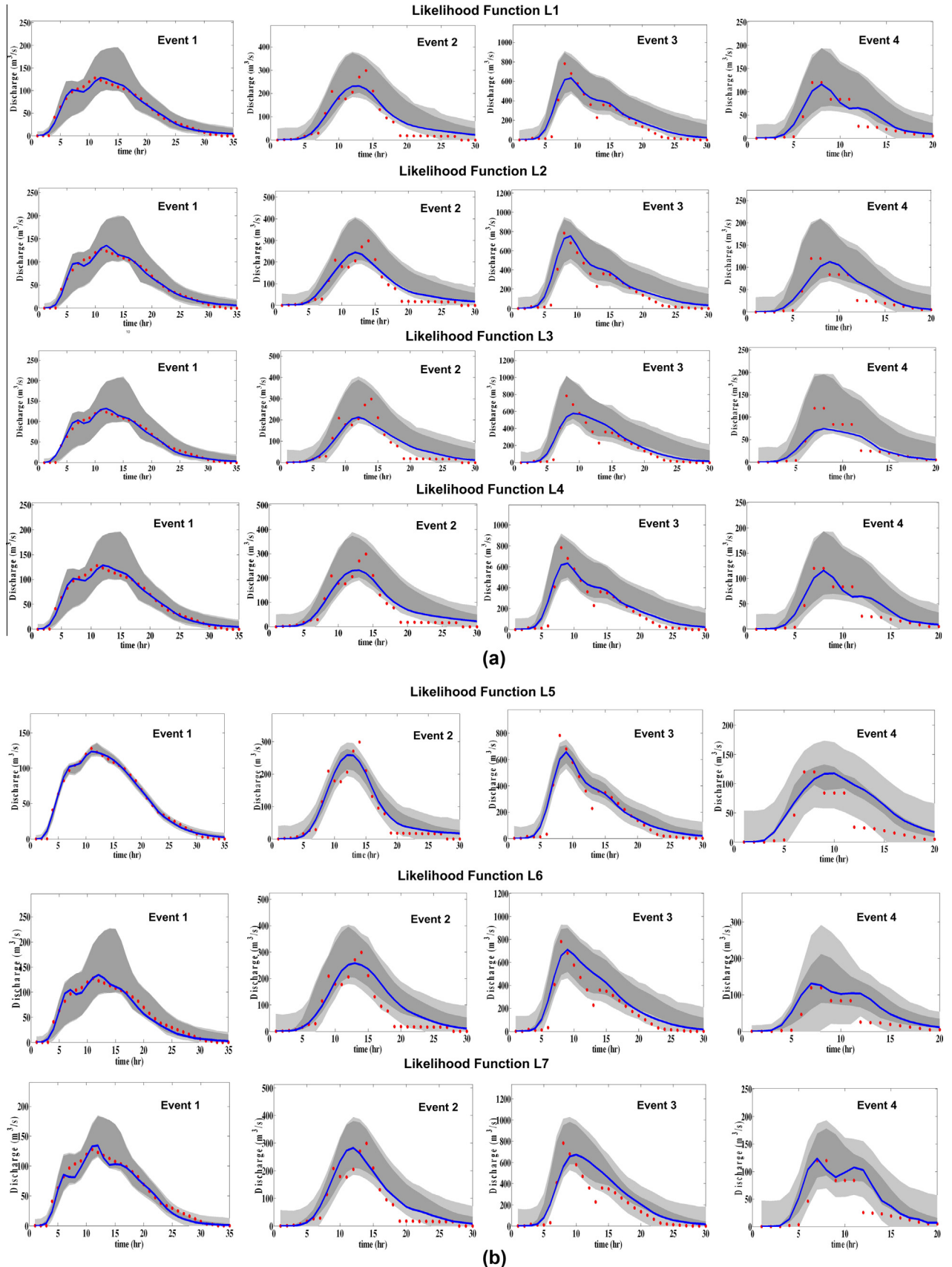
Based on Fig. 8, uncertainty bounds derived by DREAM<sub>(ZS)</sub> method are almost the same for informal Likelihood functions (L1–L4) and remain unaffected by choosing a likelihood function. Alazzy et al. (2015) also applied informal likelihood functions (L1–L4) for uncertainty assessment by the GLUE method and showed that uncertainty bounds are somewhat similar.

Fig. 9 clearly shows that R-factor (indicators of uncertainty assessment) are higher values in informal likelihood functions L1–L4, hence it is resulted they may not represent a good performance.

Moreover *R*-factor values are smaller in formal likelihood functions L5 and L7 – for all flood events (Fig. 9).

Dark gray region in Fig. 8 (corresponding to parameter uncertainty) does not bracket observed streamflow data. The gaps between the uncertainty bounds of parameter and the observed data may be originated from uncertainties in observational input–output data (forcing data) and structural inadequacy of model which is indicating that model structure and observation measurements are needed to be improved in order to achieve more accurate predictions (Laloy et al., 2010).

Based on Fig. 9, likelihood functions L5 and L7 represent a better performance, but likelihood function L5 may result in biased and unreliable estimations of parameter due to the violation of the assumptions of residual error. Thus, likelihood function L7 was used to relax common assumptions about residual errors that can provide more reliable model parameters and is prescribed for further applications.



**Fig. 8.** (a and b) Observed stream flows (dots), best simulation (maximum likelihood, solid line), 95% model prediction uncertainty bounds associated with posterior distribution of the parameter estimates (darker shaded region), and 95% total prediction uncertainty bounds (lighter shaded region).

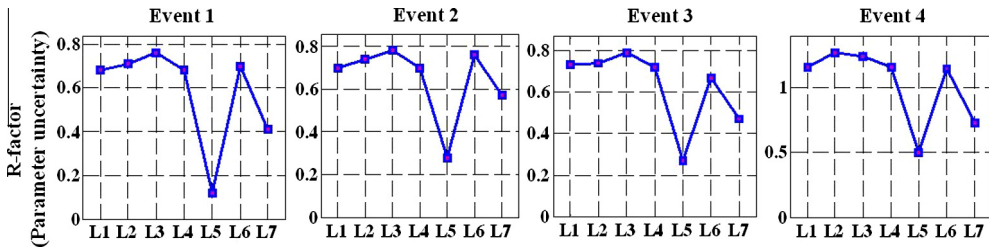


**Fig. 9.** R-factor values for parameter uncertainty assessment corresponding to different likelihood functions and for flood events in calibration and validation phases.

**Table 5**

Comparison of DREAM<sub>(ZS)</sub> performances under different likelihood functions.

Likelihood	Event	1			2			3			4		
		RMSE	KGE	NS	RMSE	KGE	NS	RMSE	KGE	NS	RMSE	KGE	NS
		L1	4.70	0.97	0.98	25.16	0.74	0.89	52.80	0.80	0.91	14.66	0.70
L2		4.96	0.96	0.99	25.39	0.74	0.89	59.17	0.66	0.89	16.49	0.72	0.79
L3		4.70	0.97	0.98	29.17	0.76	0.85	63.72	0.79	0.88	16.23	0.69	0.80
L4		4.70	0.97	0.99	25.16	0.74	0.89	52.80	0.79	0.91	14.66	0.70	0.84
L5		2.63	0.99	0.99	21.05	0.87	0.93	45.51	0.87	0.96	14.20	0.76	0.87
L6		4.45	0.98	0.98	24.53	0.82	0.90	51.20	0.83	0.93	15.62	0.73	0.85
L7		3.50	0.99	0.99	23.50	0.84	0.91	47.52	0.85	0.95	14.50	0.75	0.84

### 3.5. Comparing DREAM<sub>(ZS)</sub> performance under different likelihood functions by statistical indicators

DREAM<sub>(ZS)</sub> performances were compared under different likelihood functions by means of statistical indicators, including root-mean-square error (RMSE, Eq. (38)), Kling Gupta Efficiency (KGE, Eq. (39)), and Nash-Sutcliffe (NS, Eq. (40)) Criteria. Results showed that the smallest RMSE value in all flood events corresponded to formal likelihood function L5 (based on assumptions inherent in SLS), while L7 was in the second rank. Schoups and Vrugt (2010) verified that SLS minimizes MSE and will always yield smaller MSE values compared to the other methods, which confirms findings of the present study. Formal likelihood function L5 also better performed based on other criteria. It showed maximum values of KGE and NS for all flood events, while the second rank was of the formal likelihood function L7. Considering all statistical indicators, including RMSE, KGE and NS (Table 5) involved with 7 likelihood functions and 4 flood events, results showed that DREAM<sub>(ZS)</sub> algorithm represents a better performance significantly with formal likelihood functions L5 and L7. Although L5 and L7 represent a better performance, likelihood function L5 is highly depended on the assumptions of residual error. The residual error assumptions are clearly violated in likelihood function L5 as shown in Fig. 2, therefore, likelihood function L5 may yield unreliable parameter estimates.

Thus, likelihood function L7 was applied to relax common assumptions about residual errors that can provide reliable parameters of model and can therefore be recommended.

## 4. Conclusions

Evaluation of residual error assumptions for the first three events used in the calibration period showed that assumptions of residual error are clearly violated in likelihood function L5.

Using AR – 1 model incorporated into the formulation of the log-likelihood function after Box-Cox transformation removed temporal autocorrelation of residuals.

The results of cumulative distributions of parameters showed that choosing likelihood function can directly affect parameter

uncertainty analysis by using DREAM<sub>(ZS)</sub> method. A Likelihood function strongly affects the sensitivity of parameters and sensitivities of parameters were not the same for different likelihood functions.

The results of cumulative distributions of parameters and Kolmogorov-Smirnov test statistic (D) showed that formal likelihood functions L5 and L7 almost have completely different influence on sensitivity of parameters in comparison with the other likelihood functions for most of the parameters.

Most of the parameters were better defined by formal likelihood functions L5 and L7 and showed a high sensitivity to model performance. Therefore, they have less uncertainty and can be considered as easily identifiable parameters.

Posterior distributions of CN1–CN7 obtained by informal likelihood functions (L1–L4) and formal likelihood function L6 did not change significantly in comparison with their prior distributions, which present more uncertainty.

On the contrary, ones obtained by formal likelihood functions L5 and L7 were better defined for most parameters and had less uncertainty.

95% total prediction uncertainty ranges bracketed most of the observed flows. Totally it should be noted R-factors are higher values in informal likelihood functions L1–L4, hence it resulted they may not represent a good performance.

Moreover R-factor values are smaller in formal likelihood functions L5 and L7, hence L5 and L7 may represent a better performance.

Parameter uncertainty bounds do not bracket observed streamflow data. It may be originated from uncertainties in observational input–output data (forcing data) and structural inadequacy of model.

Considering all performance criteria, including RMSE, KGE and NS involved with 7 likelihood functions and 4 flood events, results showed that DREAM<sub>(ZS)</sub> algorithm represents a better performance with formal likelihood functions L5 and L7. Although L5 and L7 represent a better performance, likelihood function L5 is highly depended on the assumptions of residual error. In this study, the assumptions of residual error were clearly violated and likelihood function L5 may result in biased and unreliable estimations of parameter. Thus, formal likelihood function L7 was used to relax

common assumptions about residual errors that can provide reliable parameters of model and is prescribed for further applications.

The gaps between parameter uncertainty bounds and the observed data may demonstrate uncertainties of observational input (forcing) and output data and structural inadequacy of model indicating that model structure and observation measurements are needed to be improved in order to achieve more accurate predictions.

This paper disregarded rainfall data error while it may be dominant in many catchments due to significant spatial and temporal variability of rainfall fields. It seems that rainfall forcing error should be considered in uncertainty assessment of HMS model in future works. Ignoring errors of the input variables affects the structure of parameter uncertainty and confidence limits of the parameters in calibration of hydrologic models, and may lead to biased predictions (Kavetski et al., 2002, 2006a). In the future, an inference method should be employed to explicitly address the role of forcing data (precipitation) and output measurement errors, this could allow for a more accurate evaluation of model structural errors.

## Acknowledgments

The authors are thankful to Dr. Jasper A. Vrugt for providing the code for DREAM<sub>(ZS)</sub> algorithm. Also, the help of Bahareh kamali in providing data and information on the case study are appreciated. Also, we wish to thank the anonymous reviewers and the associate editor and Prof. Andras Bardossy for their helpful comments and suggestions that improved the quality of this paper.

## Appendix A. Supplementary material

Supplementary data associated with this article can be found, in the online version, at [10.1016/j.jhydrol.2016.06.022](https://doi.org/10.1016/j.jhydrol.2016.06.022).

## References

- Abbaspour, K.C., 2011. User Manual for SWAT-CUP4, SWAT Calibration and Uncertainty Programs. Swiss Federal Institute of Aquatic Science and Technology, Eawag, Duebendorf, Switzerland (103 pp.).
- Abebe, N.A., Ogden, F.L., Pradhan, N.R., 2010. Sensitivity and uncertainty analysis of the conceptual HBV rainfall-runoff model: implications for parameter estimation. *J. Hydrol.* 389, 301–310.
- Ajami, N.K., Duan, Q., Sorooshian, S., 2007. An integrated hydrologic Bayesian multimodel combination framework: confronting input, parameter, and model structural uncertainty in hydrologic prediction. *Water Resour. Res.* 43. <http://dx.doi.org/10.1029/2005WR004745>, W01403.
- Alazzy, A.A., Lü, H., Zhu, Y., 2015. Assessing the uncertainty of the Xinjiang rainfall-runoff model: effect of the likelihood function choice on the GLUE method. *J. Hydrol. Eng.* 20 (10), 04015016.
- Aron, G., Miller, A.C., Lakatos, D.F., 1997. Infiltration Formula Based on SCS Curve Number. *J. Irrig. Drain. Div.* 103 (4), 419–427.
- Baltas, E.A., Dervos, N.A., Mimikou, M.A., 2007. Technical note: Determination of SCS initial abstraction ratio in an experimental watershed in Greece. *Hydrol. Earth Syst. Sci.* 11 (6), 1825–1829.
- Bartlett, M.S., 1947. The use of transformations. *Biometrics* 3 (1), 39–52.
- Bates, B.C., Campbell, E.P., 2001. A Markov Chain Monte Carlo scheme for parameter estimation and inference in conceptual rainfall-runoff modeling. *Water Resour. Res.* 37 (4), 937–947.
- Beven, K.J., 2006. A manifesto for the enquiringly thesis. *J. Hydrol.* 320, 18–36.
- Beven, K.J., Binley, A.M., 1992. The future of distributed models: model calibration and uncertainty prediction. *Hydrol. Process.* 6 (3), 279–298.
- Beven, K., Smith, P.J., Freer, J.E., 2008. So just why would a modeler choose to be incoherent. *J. Hydrol.* 354, 15–32.
- Blasone, R.S., 2007. Parameter Estimation and Uncertainty Assessment in Hydrological Modelling Ph.D. Thesis. Institute of Environment & Resources, Technical University of Denmark (55 pp.).
- Box, G., Cox, D., 1964. An analysis of transformations. *J. R. Stat. Soc. B* 26 (2), 211–252.
- Box, G.E.P., Tiao, G.C., 1992. Bayesian Inference in Statistical Analysis. Wiley-Interscience, New York, USA (608 pp.).
- Cheng, Q.B., Chen, X., Xu, C.Y., Reinhardt-Imjela, C., Schulte, A., 2014. Improvement and comparison of likelihood functions for model calibration and parameter uncertainty analysis within a Markov chain Monte Carlo scheme. *J. Hydrol.* 519, 2202–2214.
- Chiew, F., McMahon, T., 1994. Application of the daily rainfall-runoff model Modhydrolog to 28 Australian catchments. *J. Hydrol.* 153 (1–4), 383–416.
- Chow, V.T., Maidment, D.R., Mays, L.W., 1988. Applied Hydrology. McGraw Inc, New York, USA (502, Table 15.1.2 SCS lag Equation).
- DeChant, C.M., Moradkhani, H., 2012. Examining the effectiveness and robustness of sequential data assimilation methods for quantification of uncertainty in hydrologic forecasting. *Water Resour. Res.* 48. <http://dx.doi.org/10.1029/2011WR011011>, W04518.
- Dotto, C.B.S., Kleidorfer, M., Deletic, A., Rauch, W., McCarthy, D.T., Fletcher, T.D., 2011. Performance and sensitivity analysis of stormwater models using a Bayesian approach and long-term high resolution data. *Environ. Model. Softw.* 26 (10), 1225–1239.
- Duan, Q., 1991. A Global Optimization Strategy for Efficient and Effective Identification of Calibration Models Ph.D. thesis. Department of Hydrology and Water Resources. University of Arizona, Tucson.
- Durbin, J., Watson, G.S., 1971. Testing for serial correlation in least squares regression. *Biom.* 59 (1), 1–19.
- Fenicia, F., Savenije, H.H.G., Matgen, P., Pfister, L., 2007. A comparison of alternative multiobjective calibration strategies for hydrological modeling. *Water Resour. Res.* 43. <http://dx.doi.org/10.1029/2006WR005098>, W03434.
- Freedman, V.L., Lopes, V.L., Hernandez, M., 1998. Parameter identifiability for catchment-scale erosion modelling: a comparison of optimization algorithms. *J. Hydrol.* 207, 83–97.
- Freer, J., Beven, K.J., Ambroise, B., 1996. Bayesian estimation of uncertainty in runoff prediction and the value of data: an application of the GLUE approach. *Water Resour. Res.* 32, 2161–2173.
- Freni, G., Mannina, G., Viviani, G., 2009. Uncertainty in urban stormwater quality modelling: the influence of likelihood measure formulation in the GLUE methodology. *Sci. Total Environ.* 408 (1), 138–145.
- Gao, G.Y., Fu, B.J., Lu, Y.H., Liu, Y., Wang, S., Zhou, J., 2012. Coupling the modified SCS-CN and RUSLE models to simulate hydrological effects of restoring vegetation in the Loess Plateau of China. *Hydrol. Earth Syst. Sci.* 16 (7), 2347–2364.
- Gelman, A., Rubin, D.B., 1992. Inference from iterative simulation using multiple sequences. *Stat. Sci.* 7 (4), 457–472.
- Gupta, H.V., Kling, H., Yilmaz, K.K., Martinez, G.F., 2009. Decomposition of the mean squared error and NSE performance criteria: implications for improving hydrological modeling. *J. Hydrol.* 377 (1), 80–91.
- He, J., Jones, J.W., Graham, W.D., Dukes, M.D., 2010. Influence of likelihood function choice for estimating crop model parameters using the generalized likelihood uncertainty estimation method. *Agric. Syst.* 103, 256–264. <http://dx.doi.org/10.1016/j.agys.2010.01.006>.
- Heidari, A., Saghafian, B., Maknoon, R., 2006. Assessment of flood forecasting lead time based on generalized likelihood uncertainty estimation. *Stoch. Environ. Res. Risk Assess.* 20 (5), 363–380.
- Iran Water Research Institute, Water Resources Department (IWRI), 2008. Report on Hydrologic Model Calibration: Gorganroud Flood Warning System Project. Tehran, Iran (in Persian).
- Jin, X.L., Xu, C.Y., Zhang, Q., Singh, V.P., 2010. Parameter and modeling uncertainty simulated by GLUE and a formal Bayesian method for a conceptual hydrological model. *J. Hydrol.* 383 (3–4), 147–155.
- Kamali, B., Mousavi, S.J., Abbaspour, K.C., 2013. Automatic calibration of HEC-HMS using single-objective and multi-objective PSO algorithms. *Hydrol. Process.* 27 (26), 4028–4042.
- Kavetski, D., Franks, S.W., Kuczera, G., 2002. Confronting input uncertainty in environmental modeling. In: Duan, Q., Gupta, H.V., Sorooshian, S., Rousseau, A.N., Turcotte, R. (Eds.), Calibration of Watershed Models, Water Science and Application, vol. 6. American Geophysical Union, Washington, DC, pp. 48–68.
- Kavetski, D., Kuczera, G., Franks, S.W., 2006a. Bayesian analysis of input uncertainty in hydrological modeling: 1. Theory. *Water Resour. Res.* 42. <http://dx.doi.org/10.1029/2005WR004368>, W03407.
- Kavetski, D., Kuczera, G., Franks, S.W., 2006b. Bayesian analysis of input uncertainty in hydrological modeling: 2. Application. *Water Resour. Res.* 42. <http://dx.doi.org/10.1029/2005WR004376>, W03408.
- Kool, J.B., Parker, J.C., 1988. Analysis of the inverse problem for transient unsaturated flow. *Water Resour. Res.* 24 (6), 817–830.
- Koskela, J.J., Croke, B.W.F., Koivusalo, H., Jakeman, A.J., Kokkonen, T., 2012. Bayesian inference of uncertainties in precipitation-streamflow modeling in a snow affected catchment. *Water Resour. Res.* 48 (11). <http://dx.doi.org/10.1029/2011WR011773>, W11513.
- Kousari, M.R., Malekinezhad, H., Ahani, H., Asadi Zarch, M.A., 2010. Sensitivity analysis and impact quantification of the main factors affecting peak discharge in the SCS curve number method: an analysis of Iranian watersheds. *Quat. Int.* 226, 66–74.
- Kuczera, G., 1983. Improved parameter inference in catchment models: 1. Evaluating parameter uncertainty. *Water Resour. Res.* 19 (5), 1151–1162.
- Kuczera, G., Parent, E., 1998. Monte Carlo assessment of parameter uncertainty in conceptual catchment models: the Metropolis algorithm. *J. Hydrol.* 211, 69–85.
- Kuczera, G., Kavetski, D., Franks, S., Thyre, M., 2006. Towards a Bayesian total error analysis of conceptual rainfall-runoff models: characterizing model error using storm-dependent parameters. *J. Hydrol.* 331, 161–177. <http://dx.doi.org/10.1016/j.jhydrol.2006.05.010>.
- Laloy, E., Fasbender, D., Bielders, C.L., 2010. Parameter optimization and uncertainty analysis for plot-scale continuous modeling of runoff using a formal Bayesian approach. *J. Hydrol.* 380, 82–93.

- Li, L., Xia, J., Xu, C.Y., Singh, V.P., 2010. Evaluation of the subjective factors of the GLUE method and comparison with the formal Bayesian method in uncertainty assessment of hydrological models. *J. Hydrol.* 390, 210–221.
- Liu, Y., Gupta, H.V., 2007. Uncertainty in hydrologic modeling: toward an integrated data assimilation framework. *Water Resour. Res.* 43. <http://dx.doi.org/10.1029/2006WR005756>, W07401.
- Makowski, D., Wallach, D., Tremblay, M., 2002. Using a Bayesian approach to parameter estimation: comparison of the GLUE and MCMC methods. *Agron.* 22 (2), 191–203.
- Mantovan, P., Todini, E., 2006. Hydrological forecasting uncertainty assessment: incoherence of the GLUE methodology. *J. Hydrol.* 330, 368–381.
- Marshall, L., Nott, D., Sharma, A., 2004. A comparative study of Markov chain Monte Carlo methods for conceptual rainfall-runoff modeling. *Water Resour. Res.* 40. <http://dx.doi.org/10.1029/2003WR002378>, W02501.
- Massey, F.J., 1951. The Kolmogorov-Smirnov test for goodness of fit. *J. Am. Stat. Assoc.* 46 (253), 68–78.
- McMichael, C.E., Hope, A.S., Loaiciga, H.A., 2006. Distributed hydrological modeling in California semi-arid shrublands: MIKE-SHE model calibration and uncertainty estimation. *J. Hydrol.* 317 (3–4), 307–324.
- McMillan, H., Clark, M., 2009. Rainfall-runoff model calibration using informal likelihood measures within a Markov chain Monte Carlo sampling scheme. *Water Resour. Res.* 45 (W04418). <http://dx.doi.org/10.1029/2007WR007288>, 2008W.
- Mousavi, S.J., Abbaspour, K.C., Kamali, B., Amini, M., Yang, H., 2012. Uncertainty-based automatic calibration of HEC-HMS model using sequential uncertainty fitting approach. *J. Hydroinform.* 14 (2), 286–309.
- Nash, J.E., Sutcliffe, J.V., 1970. River flow forecasting through the conceptual model. Part 1: a discussion of principles. *J. Hydrol.* 10 (3), 282–290.
- Natural Resources and Watershed Management Administration of Golestan. 2007. Report on: Gorganroud Watershed. Gorgan, Iran (In Persian).
- Ponce, V.M., Hawkins, R.H., 1996. Runoff curve number: has it reached maturity? *J. Hydrol. Eng.* 1 (1), 11–19.
- Pourreza-Bilondi, M., Akhond Ali, A.M., Ghahraman, B., 2012. Parameters uncertainty analysis in distributed single-event rainfall-runoff model with MCMC approach. *Iran. Water Res. J.* 6 (11), 165–173 (In Persian).
- Pourreza-Bilondi, M., Abbaspour, K.C., Ghahraman, B., 2013. Application of three different calibration-uncertainty analysis methods in a semi-distributed rainfall-runoff model application. *Middle-East J. Sci. Res.* 15 (9), 1255–1263.
- Rafiee Sardouei, E., Rostami, N., Khalighi Sigaroudi, S., Taheri, S., 2012. Calibration of loss estimation methods in HEC-HMS for simulation of surface runoff (Case Study: Amirkabir Dam Watershed, Iran). *Adv. Environ. Biol.* 6 (1), 343–348.
- Reichert, P., Mieleitner, J., 2009. Analyzing input and structural uncertainty of nonlinear dynamic models with stochastic, time-dependent parameters. *Water Resour. Res.* 45. <http://dx.doi.org/10.1029/2009WR007814>, W10402.
- Renard, B., Kavetski, D., Leblois, E., Thyer, M., Kuczera, G., Franks, S.W., 2011. Toward a reliable decomposition of predictive uncertainty in hydrological modeling: characterizing rainfall errors using conditional simulation. *Water Resour. Res.* 47. <http://dx.doi.org/10.1029/2011WR010643>, W11516.
- Rings, J., Vrugt, J.A., Schoups, G., Huisman, J.A., Vereecken, H., 2012. Bayesian model averaging using particle filtering and Gaussian mixture modeling: theory, concepts, and simulation experiments. *Water Resour. Res.* 48. <http://dx.doi.org/10.1029/2011WR011607>, W05520.
- Salamon, P., Feyen, L., 2009. Assessing parameter, precipitation, and predictive uncertainty in a distributed hydrological model using sequential data assimilation with the particle filter. *J. Hydrol.* 376, 428–442.
- Schoups, G., Vrugt, J.A., 2010. A formal likelihood function for parameter and predictive inference of hydrologic models with correlated, heteroscedastic and non-Gaussian errors. *Water Resour. Res.* 46, W10531.
- Schoups, G., Vrugt, J.A., Fenicia, F., van de Giesen, N.C., 2010. Corruption of accuracy and efficiency of Markov chain Monte Carlo simulation by inaccurate numerical implementation of conceptual hydrologic models. *Water Resour. Res.* 46 (10). <http://dx.doi.org/10.1029/2009WR008648>, W10530.
- SCS (Soil Conservation Service), 1972. Estimation of Direct Runoff from Storm Rainfall. Soil Conservation Service. National Engineering Hand-Book. Section 4. Hydrology. U.S. Dept. of Agriculture. Washington, DC, pp. 1–30.
- Shafiei, M., Ghahraman, B., Saghabian, B., Davary, K., Pande, S., Vazifedoust, M., 2014. Uncertainty assessment of the agro-hydrological SWAP model application at field scale: a case study in a dry region. *Agric. Water Manage.* 146 (1), 324–334.
- Smith, P.J., Beven, K., Tawn, J.A., 2008. Informal likelihood measures in model assessment: theoretic development and investigation. *Adv. Water Res.* 31 (8), 1087–1100.
- Sorooshian, S., Dracup, J.A., 1980. Stochastic parameter estimation procedures for hydrologic rainfall-runoff models: correlated and heteroscedastic error cases. *Water Resour. Res.* 16 (2), 430–442.
- Sorooshian, S., Gupta, V.K., 1983. Automatic calibration of conceptual rainfall-runoff models: the question of parameter observability and uniqueness. *Water Resour. Res.* 19 (1), 251–259.
- Sorooshian, S., Duan, Q., Gupta, V.K., 1993. Calibration of rainfall-runoff models: application of global optimization to the Sacramento soil moisture accounting model. *Water Resour. Res.* 29 (4), 1185–1194.
- Stedinger, J.R., Vogel, R.M., Lee, S.U., Batchelder, R., 2008. Appraisal of the generalized likelihood uncertainty estimation (GLUE) method. *Water Resour. Res.* 44. <http://dx.doi.org/10.1029/2008WR006822>, W00B06.
- Straub, T.D., Melching, C.S., Kocher, K.E., 2000. Equations for Estimating Clark Unit-Hydrograph Parameters for Small Rural Watersheds in Illinois. U.S. Geological Survey, Water Resources Investigations Report 00-4184, 36pp.
- ter Braak, C.J.F., Vrugt, J.A., 2008. Differential evolution Markov chain with snooker updater and fewer chains. *Stat. Comput.* 18 (4), 435–446.
- Thyer, M., Renard, B., Kavetski, D., Kuczera, G., Franks, S.W., Srikanthan, S., 2009. Critical evaluation of parameter consistency and predictive uncertainty in hydrological modeling: a case study using Bayesian total error analysis. *Water Resour. Res.* 45. <http://dx.doi.org/10.1029/2008WR006825>, W00B14.
- USACE, 2000. HEC-HMS Technical Reference Manual. US Army Corps of Engineers, Hydrologic Engineering Center, Davis, California (158 pp.).
- USACE, 2013. HEC-HMS User's Manual. US Army Corps of Engineers, Hydrologic Engineering Center, Davis, California (442 pp.).
- Vrugt, J.A., Bouten, W., 2002. Validity of first-order approximations to describe parameter uncertainty in soil hydrologic models. *Soil Sci. Soc. Am. J.* 66 (6), 1740–1751.
- Vrugt, J.A., Robinson, B.A., 2007. Treatment of uncertainty using ensemble methods: comparison of sequential data assimilation and Bayesian model averaging. *Water Resour. Res.* 43. <http://dx.doi.org/10.1029/2005WR004838>, W01411.
- Vrugt, J.A., Sadegh, M., 2013. Toward diagnostic model calibration and evaluation: Approximate Bayesian computation. *Water Resour. Res.* 49, 4335–4345. <http://dx.doi.org/10.1002/wrcr.20354>.
- Vrugt, J.A., Gupta, H.V., Bouten, W., Sorooshian, S., 2003. A Shuffled Complex Evolution Metropolis algorithm for optimization and uncertainty assessment of hydrologic parameter estimation. *Water Resour. Res.* 39 (8), 1201.
- Vrugt, J.A., ter Braak, C.J.F., Clark, M.P., Hyman, J.M., Robinson, B.A., 2008. Treatment of input uncertainty in hydrologic modeling: Doing hydrology backward with Markov chain Monte Carlo simulation. *Water Resour. Res.* 44 (12), W00B09.
- Vrugt, J.A., ter Braak, C.J.F., Diks, C.G.H., Robinson, B.A., Hyman, J.M., Higdon, D., 2009a. Accelerating Markov Chain Monte Carlo simulation using self-adaptive differential evolution with randomized subspace sampling. *Int. J. Nonlin. Sci. Numer. Simul.* 10 (3), 273–290.
- Vrugt, J.A., ter Braak, C.J.F., Gupta, H.V., Robinson, B.A., 2009b. Equifinality of formal (DREAM) and informal (GLUE) Bayesian approaches in hydrologic modeling? *Stoch. Environ. Res. Risk Assess.* 23 (7), 1011–1026.
- Vrugt, J.A., ter Braak, C.J.F., Diks, C.G.H., Schoups, G., 2013. Advancing hydrologic data assimilation using particle Markov chain Monte Carlo simulation: theory, concepts and applications. *Adv. Water Resour.*, Anniversary Issue – 35 Years 51, 457–478. <http://dx.doi.org/10.1016/j.advwatres.2012.04.002>.
- Wagener, T., Lees, M.J., Wheater, H.S., 2002. A toolkit for the development and application of parsimonious hydrological models. In: Singh, V.P., Frevert, D., Meyer (Eds.), Mathematical Models of Small Watershed Hydrology, vol. 2. Water Resources Publications, LLC, USA.
- Wang, Y., Huang, M.B., 2008. Application of the SCSCN method on runoff estimation in small watershed on Loess Plateau. *Sci. Soil Water Conserv. (in Chinese)* 6 (6), 87–91.
- Willmott, C.J., Ackleson, S.G., Davis, R.E., Feddema, J.J., Klink, K.M., Legates, D.R., O'Donnell, J., Rowe, C.M., 1985. Statistics for the evaluation and comparison of models. *J. Geophys. Res.* 90 (C5), 8995–9005.
- Wöhling, T., Vrugt, J.A., 2011. Multiresponse multilayer vadose zone model calibration using Markov chain Monte Carlo simulation and field water retention data. *Water Resour. Res.* 47. <http://dx.doi.org/10.1029/2010WR009265>, W04510.
- Xiao, B., Wang, Q.H., Fan, J., Han, F.P., Dai, Q.H., 2011. Application of the SCS-CN model to runoff estimation in a small watershed with high spatial heterogeneity. *Pedosph.* 21 (6), 738–749.
- Yang, J., Reichert, P., Abbaspour, K.C., Yang, H., 2007a. Hydrological modelling of the Chaohe Basin in China: statistical model formulation and Bayesian inference. *J. Hydrol.* 340, 167–182.
- Yang, J., Reichert, P., Abbaspour, K.C., 2007b. Bayesian uncertainty analysis in distributed hydrological modelling: a case study in the Thur River basin (Switzerland). *Water Resour. Res.* 43, W10401.